Distribution of the entanglement entropies of non-ergodic quantum states

Devanshu Shekhar and Pragya Shukla*

Department of Physics, Indian Institute of Technology,

Kharagpur-721302, West Bengal, India

(Dated: December 11, 2024)

Abstract

Beginning from an ensemble of pure bipartite states typically characterized by arbitrary, non-maximum entanglement, we seek the route to achieve an ensemble with maximum entanglement for a typical state. Our approach is based on the consideration of a pure quantum state, with its components non-identical but independent Gaussian distributed in a bipartite product basis. A change of ensemble parameters leads to a variation of the entanglement entropy distribution from its initial to maximum state. We show that the variation can be described by a common mathematical formulation for a wide range of initial ensembles, with a function of all ensemble parameter governing the variation. The information provides an alternative approach to quantum purification and error correction for communication through noisy quantum channels.

*Corresponding author, E-Mail: shukla@phy.iitkgp.ac.in

I. INTRODUCTION

Quantum entanglement is a unique phenomenon, relevant not only for fundamental considerations but also for its increasing viability as a resource for various quantum information processes [1, 2]. A maximally entangled state is an ideal requirement for a quantum information process. While entangled states can be produced under controlled experiments, unavoidable noise in such control operations, thermal fluctuations as well as interactions with an uncontrollable environment leave the desired state with a non–unit fidelity. The search for routes to protect the entangled states and the information carried by them over noisy quantum channels has led to various tools e.g. quantum error correction [2], entanglement purification [1] etc. Specific limitations associated with previous tools however motivate search for the new ones. The primary objective of present study is to suggest a new tool which results in an ensemble of maximum entangled states beginning from an ensemble of separable or partially entangled states.

Almost all protocols for maintenance of the high fidelity entanglement for practical applications require consideration of an ensemble of states. For example, for long-range quantum communication, a route to protect quantum information is by its encoding, through entanglement, in a concatenated quantum error correcting code. The transmission of the encoded quantum state through a noisy channel is followed by an error correction step that involves

decoding and measurements. The noisy passage however randomizes the encoded state, leaving it best described by an ensemble. For any efficient decoding, it is relevant to know a priori the entanglement distribution of the ensemble. An alternative quantum communication route is based on entanglement purification or distillation: it manipulates an ensemble of noisy, non-maximally entangled states so as to leave behind only a fewer number of copies with a reduced amount of noise. The entanglement of the total ensemble is concentrated or distilled in a few copies thereby containing a larger amount of entanglement and have higher fidelity.

In real applications, noise is usually unavoidable. It is thus natural to query whether it is possible to harness the noise to favour the quantum information processes? More clearly, is it possible to start from a pure state with arbitrary entanglement and apply noisy operations to convert it into an ensemble of fully entangled states? An additional issue arises from a wide range of system conditions e.g. from external noise (changing environment) which can lead to ensembles with different types and strength of randomness. It will therefore be useful to have a protocol that can control the dependence collectively i.e through a single function of all system parameters. The present study pursues the above queries by theoretically analysing the entanglement distribution for a wide range of ensembles of quantum states and seek a common mathematical formulation for its dynamics if feasible. Our results are encouraging: we find that such a formulation indeed exists for pure states with Gaussian distributed components in a bipartite basis. The formulation in turn helps to identify the path the protocol can opt for to achieve maximum entangled ensemble starting from a non-maximum entangled ensemble.

The standard representation of a quantum state is based on its components describing the overlap of the state with basis vectors in a physically motivated basis. It is however technically non-trivial, almost impossible, usually, to determine the components exactly if the state is that of a many-body system [3]. A lack of exact information about the Hamiltonian matrix elements e.g. due to disorder or complicated interactions usually manifests through a randomization of the eigenstate components with often non-negligible system-specific fluctuations at a local scale. Also indicated by previous studies on many body systems, a maximally entangled state displays ergodic dynamics in the single body product basis. In contrast, a separable state tends to localize in this basis. Between these two extremes, lies a whole range of states i.e non-maximally entangled states with non-ergodic dynamics. In-

deed an ensemble of such states appears in general in any practical quantum information process; this makes it relevant to determine the distribution of the entanglement measures over the ensemble for a given set of system conditions. The information is desirable e.g. to determine an appropriate purification procedure, or whether a controlled variation of the system conditions can lead to an ensemble of fully entangled states.

For a clear exposition of our ideas, the present study is confined to the cases with $2nd$ rank state tensor of a pure bipartite state, hereafter referred as the state matrix or just C-matrix. We note while the fundamental aspects of the entanglement e.g. many body localization studies require insights into multipartite entanglement, its application aspects e.g. security of quantum communication is often based on a shared state between two parties. This encourages us to confine the present analysis to bipartite entanglement.

The standard entanglement measures for a pure bipartite state can in principle be obtained from the eigenvalues of the reduced density matrix. Previous studies in this context have been confined to ergodic states; the related reduced density matrix can then be well-modelled by the basis invariant Wishart random matrix ensembles [4–15]. But, as mentioned above, a typical many-body state, need not be maximally entangled and can also exhibit different degree of localization *e.g.,* fully or partially localized or extended based on system parameters like disorder strength and dimensionality. The reduced density matrix for such cases belongs to a general class of Wishart random matrix ensembles where system-dependence appears through distribution parameters of the matrix elements [16]. This in turn affects the distribution of the Schmidt eigenvalues and can thereby cause fluctuations in the entanglement measures too, an aspect which has been neglected so far to best of our knowledge. As shown in a previous study [17], the probability density of the Schmidt eigenvalues undergoes a diffusive dynamics with changing system condition, with its variation governed by a measure referred as complexity parameter. In the present work, we apply the formulation to derive the probability densities of the entanglement measures and their growth with changing system conditions.

The paper is organized as follows. In [17], we derived the complexity parameter formulation of the probability density of the Schmidt eigenvalues of a bipartite pure state represented by a multiparametric Wishart ensemble. As the information is needed to derive the distributions of the entanglement entropies, it is briefly reviewed in section II. Sections III and IV contain the probability density formulation for the moments of the Schmidt eigenvalues,

with primary focus on the purity, and Von Neumann entropy, respectively. For purpose of clarity, the details of the derivations are presented in the appendices. The numerical analysis presented in section V verifies our theoretical predictions. We conclude in section VI with a brief summary of our results, their relevance and open questions.

II.   STATE MATRIX ENSEMBLE FOR A PURE STATE

An arbitrary pure state $|\Psi\rangle$ of a composite system, consisting of two subsystems A and B can be written as $|\Psi\rangle = \sum_{i,j} C_{ij} |a_i\rangle |b_j\rangle$, with $|a_i\rangle$ and $|b_j\rangle$, $i = 1 \ldots N_a, j = 1 \ldots N_b$ as the orthogonal basis states in the subspaces of A and B respectively, forming a $N_a \times N_b$ product basis $|a_i\rangle |b_j\rangle$.

The reduced density matrix ρ_A can then be obtained from the density operator $\rho = |\Psi\rangle\langle\Psi|$ by a partial trace operation on B-subspace, $\rho_A \equiv C\,C^\dagger$, subjected to a fixed trace constraint $\text{Tr}\rho_A = 1$. As C consists of the coefficients (components) of the state Ψ, we refer it as the state matrix or just C-matrix. A knowledge of the eigenvalues λ_n with $n = 1 \ldots N_a$ of ρ_A, also known as Schmidt eigenvalues, leads to various entanglement entropies, defined as

$$R_\alpha = \frac{1}{1-\alpha}\ln \text{Tr}(\rho_A^\alpha) = \frac{1}{1-\alpha}\ln \sum_n \lambda_n^\alpha. \tag{1}$$

with the eigenvalues subjected to the trace constraint $\sum_{n=1}^N \lambda_n = 1$, $\alpha \to 1$ referring to the Von Neumann entropy and $\alpha > 1$ as the Rényi entropies.

A separable pure state of a bipartite system can in general be written as $|\Psi\rangle = |\phi_a\rangle |\phi_b\rangle$ with $|\phi_a\rangle = \sum_i a_i |a_i\rangle$ and $|\phi_b\rangle = \sum_j b_j |b_j\rangle$; a typical element of C matrix can then be written as $C_{ij} = a_i b_j$. This in turn gives only one of the Schmidt eigenvalues as one and all others zero (due to unit trace constraint) and thereby leads to $R_{alpha} = 0$. On the contrary, an ergodic pure state corresponds to almost all C_{ij} of the same order and thereby corresponding Schmidt eigenvalues of the same order: $\lambda_n \sim \frac{1}{N}$ for $n = 1 \ldots N$ again subjected to constraint $\sum_{n=1}^N \lambda_n = 1$. This in turn leads to $R_\alpha \sim \log N$ [4]. The matrix elements of a C matrix for a generic non-ergodic state in general lie between the two limits.

As mentioned in section I, the transmission of a state through a noisy quantum channel can cause randomization of its components. For example, in quantum error correction codes, the state is usually coupled with a few known ancilla states resulting in a multipartite

state. It is then made to pass through a noisy channel, resulting in a randomization of its components. Even if the original state is a non-random one, the state emerging from the noisy channels is best described by an ensemble. This can be further explained by following prototypical example (later referred as example 1). Consider a pure qubit state in the computational basis i.e $|\Psi\rangle = \alpha|0\rangle + \gamma|1\rangle$. It passes through a noisy channel described by a unitary operator $U = \begin{pmatrix} a & b \\ c & d \end{pmatrix}$ with a, b, c, d Gaussian distributed with zero mean and variances $\sigma_a^2, \sigma_b^2, \sigma_c^2, \sigma_d^2$ respectively. The new state $|\Psi'\rangle = U|\Psi\rangle$ can be written as $|\Psi'\rangle = \alpha'|0\rangle + \gamma'|1\rangle$. With $\alpha' = a\alpha + b\gamma, \gamma' = c\alpha + d\gamma$ and a, b, c, d as random variables, this results in $|\Psi'\rangle$ as a random state, with its components α', γ' as Gaussian distributed:

$$\rho_f(\alpha') = \frac{1}{2\pi\sigma_a\sigma_b} \int da\, db\, \delta(\alpha' - a\alpha - b\gamma)\, e^{-\frac{a^2}{2\sigma_a^2} - \frac{b^2}{2\sigma_b^2}} \tag{2}$$

$$= \frac{\sigma_a\sigma_b\alpha}{\sqrt{\pi^3(\alpha^2\sigma_a^2 + \gamma^2\sigma_b^2)}} \exp\left[-\frac{\alpha'^2}{2\sigma_a^2\alpha^2}\left(1 - \frac{\alpha^2\sigma_a^2\gamma^2\sigma_b^2}{\alpha^2\sigma_a^2 + \gamma^2\sigma_b^2}\right)\right] \tag{3}$$

and

$$\rho_f(\gamma') = \frac{1}{2\pi\sigma_c\sigma_d} \int dc\, dd\, \delta(\gamma' - c\alpha - d\gamma)\, e^{-\frac{c^2}{2\sigma_c^2} - \frac{d^2}{2\sigma_d^2}} \tag{4}$$

$$= \frac{\sigma_c\sigma_d\alpha}{\sqrt{\pi^3(\alpha^2\sigma_c^2 + \gamma^2\sigma_d^2)}} \exp\left[-\frac{\gamma'^2}{2\sigma_c^2\alpha^2}\left(1 - \frac{\alpha^2\sigma_c^2\gamma^2\sigma_d^2}{\alpha^2\sigma_c^2 + \gamma^2\sigma_d^2}\right)\right] \tag{5}$$

The state $|\Psi'\rangle$ is now described by the ensemble $\rho_f = \rho_f(\alpha')\rho_f(\gamma')$. We note as the components of the state $|\Psi\rangle$ were chosen to be non-random, it is described by a probability density $\rho_i = \delta(\alpha' - \alpha)\delta(\gamma' - \gamma)$. The above gives rise to the query whether it is possible to change the variances $\sigma_a^2, \sigma_b^2, \sigma_c^2, \sigma_d^2$ in time t such that a typical state in the ensemble of states $|\Psi'\rangle$ turns out to be a maximally entangled one? Taking U as a $2^L \times 2^L$ random unitary matrix, the above example can also be generalized to show the randomization of a pure bipartite state of L qubits. Clearly a retrieval of the original information content of the state requires a detailed statistical analysis of the ensemble.

The randomization of the components of an eigenstate is not confined only to environmental effects. A lack of detailed information about the components (some or all) of a generic many body state in a physically motivated basis often leaves them determined only by a distribution. As a consequence, the C-matrix for the pure state is best represented by an ensemble, with latter's details subjected to the physical constraints on the state, *e.g.,* symmetry, conservation laws, dimensionality etc. We emphasize, contrary to a mixed state,

the term "ensemble" used in our analysis refers to the one arising due to a randomization of the components of a quantum state $|\Psi\rangle$ due to complexity e.g disorder or many body interactions (e.g. a determination of the components in the product basis requires multiple integrations, leading to approximations). Our analysis is confined to pure states and does not include mixed states where the notion of the ensemble appears due to experimental errors or thermal fluctuations.

We consider the pure bipartite states for which a typical C-matrix element is known only by its average and variance. Following maximum entropy hypothesis, the C-matrix ensemble can then be described by a multiparametric Gaussian ensemble [17]

$$\rho_c(C; h, b) = \mathcal{N} \exp\left[-\sum_{k,l,s} \frac{1}{2h_{kl;s}} (C_{kl;s} - b_{kl;s})^2\right] \tag{6}$$

with $\sum_{k,l,s} \equiv \sum_{k=1}^{N} \sum_{l=1}^{N_\nu} \sum_{s=1}^{\beta}$ and $\mathcal{N}$ as a normalization constant: $\mathcal{N} = \prod_{k,l,s} (2\pi h_{kl;s})^{-1/2}$. Here $\beta = 1, 2$ for real and complex matrices respectively. Also, $h \equiv [h_{kl,s}]$ and $b \equiv [b_{kl,s}]$ refer to the matrices of variances and mean values of $C_{kl;s}$. As the ensemble parameters are governed by correlations among the basis states, different choices of h and b-matrices in eq.(6) corresponds to the ensembles representing different pure states. For example, the ensemble for a separable state with $C_{i1} = a_i b_1$, $C_{ij} = 0$ for $j > 1$ (representing the state of part B localized to just one local basis state $i.e.$, $|\phi_b\rangle = |b_1\rangle$) can be modelled by eq.(6) by choosing $h_{kl;s}, b_{kl;s} \to 0$ for $l \neq 1$. The ensemble of pure ergodic states can similarly be modelled by all $h_{kl;s}$ of the same order and all $b_{kl;s}$ too $e.g.$, $h_{kl;s} \to \sigma^2$, $b_{kl;s} \to 0$. A choice of varied combinations of $h_{kl;s}, b_{kl;s}$ in general leads to the ensemble of non-ergodic states; some of them are used later in section V for numerical verification of our results.

As discussed in [17], a variation of system parameters, $e.g.$, due to some external perturbation can lead to a dynamics in the matrix space as well as in the ensemble space, former by a variation of the matrix elements and the latter by a variation of the ensemble parameters. Interestingly, following an exact route, a specific type of multi-parametric dynamics in the ensemble space ($i.e.$, a particular combination of the first order parametric derivatives of $\rho(H)$) can then be mapped to a Brownian dynamics of $\rho(H)$ in the matrix space. This in turn leads to complexity parameter governed variation of the joint probability distribution function (JPDF) of the Schmidt eigenvalues (denoted as $P_c(\lambda)$ hereafter)

$$P_c(\lambda_1, \lambda_2, \ldots, \lambda_N; Y) = \delta\left(\sum_n \lambda_n - 1\right) P_\lambda(\lambda; Y) \tag{7}$$

where $P(\lambda_1, \lambda_2, \ldots, \lambda_N; Y)$, referred as $P_\lambda(\lambda; Y)$ hereafter, satisfies following diffusion equation,

$$\frac{\partial P_\lambda}{\partial Y} = 4 \sum_{n=1}^{N} \left[\frac{\partial^2 (\lambda_n \, P_\lambda)}{\partial \lambda_n^2} - \frac{\partial}{\partial \lambda_n} \left(\sum_{m=1}^{N} \frac{\beta \lambda_n}{\lambda_n - \lambda_m} + \beta \nu - 2\gamma \lambda_n \right) P_\lambda \right] \tag{8}$$

where $\nu = (N_\nu - N_a + 1)/2$ and Y is known as the ensemble complexity parameter [16, 18–20]

$$Y = -\frac{1}{2M\gamma} \ln \left[\prod_{k,l}' \prod_{s=1}^{\beta} |(1 - 2\gamma h_{kl;s})| \, |b_{kl;s}|^2 \right] + \text{const} \tag{9}$$

with $\prod_{k,l}'$ implies a product over non-zero $b_{kl;s}$ as well as $h_{kl;s}$, with M as their total number; (for example for the case with all $h_{kl;s} \neq \frac{1}{2\gamma}$ but $b_{kl;s} = 0$, we have $M = \beta N N_\nu$ and for case with all $h_{kl;s} \neq \frac{1}{2\gamma}$ and $b_{kl;s} \neq 0$, we have $M = 2\beta N N_\nu$). Here γ is an arbitrary parameter, related to final state of the ensemble (giving the variance of matrix elements at the end of the variation) and the constant in eq.(9) is determined by the initial state of the ensemble [21]. As Y in eq.(8) appears as a time like variable, hereafter we refer the variation of P_λ described by the equation as an evolution or growth with Y as a "pseudo-time".

The above equation describes the diffusion of $P_\lambda(\lambda, Y)$, with a finite drift, from an arbitrary initial state $P_\lambda(\lambda, Y_0)$ at $Y = Y_0$. For example, if the initial ensemble $\rho_c(C)$ corresponds to that of separable quantum states, we have

$$P_\lambda(\lambda, Y_0) = \sum_{n=1}^{N} e^{-\frac{(\lambda_n - 1)^2}{2\sigma^2}} \prod_{m \neq n} \delta(\lambda_m) \tag{10}$$

In limit $\frac{\partial P_\lambda}{\partial Y} \to 0$ or $Y \to \infty$, the diffusion approaches a unique steady state:

$$P_\lambda(\lambda; \infty) \propto \prod_{m<n=1}^{N} |\lambda_m - \lambda_n|^\beta \prod_{k=1}^{N} |\lambda_k|^{2\nu\beta - 1} \, e^{-\frac{\gamma}{2} \sum_{k=1}^{N} \lambda_k} \tag{11}$$

An important point worth noting here is as follows: although the above distribution along with eq.(7) corresponds to the Schmidt eigenvalues of an ergodic state within unit trace constraint, it does not represent that of a maximally entangled state. In the latter case with Gaussian randomness, we have

$$P_\lambda(\lambda, \infty) \propto e^{-\frac{\gamma}{2} \sum_{n=1}^{N} \left(\lambda_n - \frac{\alpha_n}{N} \right)^2} \tag{12}$$

with $\sum_n \alpha_n = N$; an example of α_n satisfying the constraint in large N limit is $\alpha_n = 1$. Clearly their repulsion in eq.(11) renders it impossible for the eigenvalues to reach to the

same value $1/N$. Further we note that while all but one Schmidt eigenvalues of a separable state cluster around zero, those for maximally entangled state cluster around $1/N$. Thus while the quantum state itself may change from localized to ergodic limit, the Schmidt states *i.e.*, eigenstates of ρ_A seem to behave differently. But as the entanglement entropy for an ergodic state is almost maximum, this suggests different routes for maximum entanglement for random and non-random states.

As discussed in detail in [17, 21], the parametric variation described in eq.(8) is subject to a set of constants of dynamics. The latter arise from a mapping of the set $\{h, b\}$ of ensemble parameters (say M of them varying) to another set $\{Y, Y_2, \ldots, Y_M\}$ so that the first order partial derivatives with respect to M ensemble parameters reduces to a single partial derivative with respect to Y. The remaining parameters $Y_2, \ldots, Y_M$ play the role of constants of dynamics. As the relevance of $Y_2, \ldots Y_M$ has been discussed in detail [17, 21] and explained through examples in [22], we discuss only the role of Y in the present analysis.

III. DISTRIBUTION OF THE MOMENTS OF SCHMIDT EIGENVALUES

As eq.(1) indicates, the Rényi entropy R_k is related to the moments $S_k(\equiv \sum_n \lambda_n^k)$ of the Schmidt eigenvalues, and it is appropriate to first consider the probability density of S_k, $k > 1$, defined as

$$f_k(S_k; Y) = \int \delta \left(S_k - \sum_{n=1}^{N} \lambda_n^k \right) \ \delta \left(\sum_{n=1}^{N} \lambda_n - 1 \right) \ P_\lambda(\lambda; Y) \ \mathrm{D}\lambda \tag{13}$$

Using the product of δ-functions in the above integral, f_k can alternatively be defined in terms of the joint probability density of the moments $P_q(S_1, S_2, \ldots, S_q)$

$$f_k(S_k; Y) = \int \delta(S_1 - 1) \ P_q(S_1, \ldots, S_q; Y) \ \prod_{\substack{m=1 \\ m \neq k}}^{q} \mathrm{d}S_k. \tag{14}$$

where

$$P_q(S_1, S_2, \ldots, S_q; Y) = \int \prod_{k=1}^{q} \delta(S_k - \sum_{n=1}^{N} \lambda_n^k) \ P_\lambda(\lambda; Y) \ \mathrm{D}\lambda \tag{15}$$

For clarity purposes, here the notation $f_k(S_k)$ is reserved for the distribution of a single moment S_n and P_q to the JPDF of q such moments. Also, to avoid cluttering of presentation, henceforth we use following notations interchangeably: $\sum_n \equiv \sum_{n=1}^{N}$, $\delta \left(\sum_{n=1}^{N} \lambda_n - 1 \right) \equiv \delta_1$ and $\delta_{S_k} \equiv \delta \left(S_k - \sum_{n=1}^{N} \lambda_n^k \right)$. Also, for simplicity, hereafter we consider the case of $k = 2$.

9

A. Distribution of purity

From eq.(14), the probability density of purity S_2 can be written as

$$f_2(S_2; Y) = \int_0^\infty \delta(S_1 - 1) \, P_2(S_1, S_2; Y) \, dS_1, \tag{16}$$

where, $S_1 \equiv \sum_n \lambda_n$. We note that the δ-unction in the above acts like a filter, picking the value of $P_2(S_1, S_2; Y)$ at $S_1 = 1$. It can therefore be replaced by a narrow width function $g(S_1)$ centred at $S_1 = 1$ such that (i) the product $g(S_1)P_2(S_1, S_2; Y)$ is non-zero only in the vicinity of $S_1 = 1$, and, (ii) integrating the product over S_1 gives $g(S_1)P_2(1, S_2; Y)$. Using the definition $f_2(S_2; Y) = f_{2,\omega}(S_2; Y)$ in large ω limit, eq.(16) can now be rewritten as

$$f_{2,\omega}(S_2; Y) = \int_0^\infty g(S_1) \, P_2(S_1, S_2; Y) \, dS_1 \tag{17}$$

Differentiation of the above equation with respect to Y gives the Y-dependent growth of $f_{2,\omega}$:

$$\frac{\partial f_{2,\omega}}{\partial Y} = \int_0^\infty g(S_1) \, \frac{\partial P_2}{\partial Y} \, dS_1. \tag{18}$$

To proceed further, a knowledge of the Y- governed variation of $P_2(S_1, S_2; Y)$ is required; this can be obtained by differentiating eq.(15) for $q = 2$ with respect to Y and subsequently using eq.(8) (details discussed in *appendix* A):

$$\frac{\partial P_2}{\partial Y} = 4\frac{\partial^2 (S_2 \, P_2)}{\partial S_2 \partial S_1} + 4\frac{\partial^2 I_3}{\partial S_2^2} + \frac{\partial^2 (S_1 \, P_2)}{\partial S_1^2} + \frac{\partial (Q_2 \, P_2)}{\partial S_2} + \frac{\partial (Q_1 \, P_2)}{\partial S_1} \tag{19}$$

with $Q_2 \equiv (2\gamma S_2 - \beta(N + \nu - 1)S_1 - S_1)$, $Q_1 = 2\gamma S_1 - \frac{\beta}{2}N(N + 2\nu - 1)$ and

$$I_3 = \int \prod_{k=1}^2 \delta_{S_k} \left(\sum_n \lambda_n^3 \right) P_\lambda \, D\lambda = \int S_3 \, P_3(S_1, S_2, S_3) \, dS_3. \tag{20}$$

We note that all other terms except one in eq.(19) contain the derivatives of P_2. To reduce it as a closed form equation for P_2, we rewrite $P_3(S_1, S_2, S_3) = P(S_3|S_2, S_1) \, P_2(S_2, S_1)$. This gives $I_3 = \langle S_3 \rangle_{S_2, S_1} P_2$ where $\langle S_3 \rangle_{S_2, S_1} = \int S_3 \, P(S_3|S_2, S_1) \, dS_3$ is the "local average" *i.e.*, ensemble average of S_3 for a given S_2, S_1. Substitution of the so obtained I_3 form in eq.(19) gives now the diffusion equation for P_2 for arbitrary S_1 in a closed form.

Using eq.(19) in eq.(18), integrating by parts, and subsequently using the relation $f_{2,\omega}(S_2) \to 0$ at the integration limits $S_1 = 0, \infty$, now leads to

$$\frac{\partial f_{2,\omega}}{\partial Y} = \frac{\partial^2 f_{2,\omega}}{\partial S_2^2} + (\eta \, S_2 + b)\frac{\partial f_{2,\omega}}{\partial S_2} + d_0 \, f_{2,\omega}, \tag{21}$$

with,

$$a = 4\langle S_3 \rangle_{S_2, S_1 = 1}, \tag{22}$$

$$b = -\beta(N + \nu - 1) + 2\frac{\partial a}{\partial S_2}, \tag{23}$$

$$\eta = 2\gamma - 4 \, g_1, \tag{24}$$

$$d_0 = 4\gamma - (6 + 2\gamma - \frac{\beta}{2}NN_\nu)g_1 + g_2 + \frac{\partial^2 a}{\partial S_2^2}, \tag{25}$$

where, $g_n(S_1) \equiv \frac{1}{g}\frac{\partial^n g(S_1)}{\partial S_1^n}$ and $N_\nu = N + 2\nu - 1$. Here again the above closed form equation is obtained by approximating the product term $g(S_1) \, \langle S_3 \rangle_{S_2, S_1}$ in the following integrand by its value at $S_1 = 1$ (the peak of $g(S_1)$),

$$\int_0^\infty g(S_1) \, \langle S_3 \rangle_{S_2, S_1} \, P_2(S_1, S_2; Y) \, \mathrm{d}S_1 = \langle S_3 \rangle_{S_2, S_1 = 1} \tag{26}$$

We note $\langle S_3 \rangle$ is in general a function of Y, leaving the right side of eq.(21) Y-dependent. This makes it technically complicated to solve; further progress can however be made by noting that S_3 and S_2 change at different rates with Y, with S_3 changing much slower than S_2 and can be assumed almost constant as S_2 evolves with Y. This permits us to replace $\langle S_3 \rangle_{S_2, S_1 = 1}$ by the latter averaged over all S_2, referred as $\langle S_3 \rangle$, ignore terms $\frac{\partial a}{\partial S_2}$ and $\frac{\partial^2 a}{\partial S_2^2}$ in eq.(25) and consider a separation of variables approach to solve eq.(21).

Although in principle it is possible to proceed without considering any specific form of the limiting function $g(S_1)$, for technical clarity here we consider

$$g(S_1) = \omega \, \mathrm{e}^{-\omega \, (S_1 - 1)}. \tag{27}$$

While the above function approaches a δ-function (for $S_1 \geq 1$) in limit $\omega \to \infty$), but to act as a desired filter, it is sufficient to have its width much smaller than that of $P_2(S_1, S_2; Y)$. This in turn gives $g_n(S_1) = (-1)^n \, \omega^n$ and thereby $\eta \approx 4\omega$ (in large ω-limit and as γ a fixed constant). Further, with our primary interest in $S_1 = 1$, it is sufficient to consider the above form instead of the form $\omega \, \mathrm{e}^{-\omega \, |S_1 - 1|}$ valid for entire real line.

11

A general solution of the above equation then gives the growth of the probability density of purity from arbitrary initial condition (at $Y = Y_0$) as Y varies. But, with $\langle S_3 \rangle$ in general Y-dependent, the above equation is non-linear in Y and is technically difficult to solve. Further steps can however be simplified by considering a rescaled variable x defined as

$$x = \left(\frac{\omega}{2 \langle S_3 \rangle} \right)^{\frac{1}{2}} S_2. \tag{28}$$

Further defining $\Psi(x, Y)$ as the transformed probability, given by the relation $f_{2,\omega}(S_2, Y) = \Psi(x, Y) \frac{\mathrm{d}x}{\mathrm{d}S_2}$, eq.(21) can now be rewritten as

$$\frac{\partial \Psi}{\partial Y} = 2\omega \frac{\partial^2 \Psi}{\partial x^2} + \eta (x + b_1) \frac{\partial \Psi}{\partial x} + d_0 \Psi \tag{29}$$

where $b_1 = \frac{b}{\eta} \sqrt{\frac{\omega}{2 \langle S_3 \rangle}}$. Further, since $\eta \approx 4\omega$, we can approximate $x + b_1 \approx x$, thereby leaving the right side of the above equation Y-independent. Eq.(29) can now be solved by the separation of variables approach; as discussed in *appendix* B in detail, the general solution for arbitrary $Y - Y_0$ can be given as

$$\Psi(x; Y - Y_0) \approx e^{-x^2} \sum_{m=0}^{\infty} C_m \, {}_1F_1 \left(-\mu_m, \frac{1}{2}, x^2 \right) e^{-d_0 m (Y - Y_0)} \tag{30}$$

where, ${}_1F_1(a, b, z)$ is the *Kummer's* Hypergeometric function [23] with

$$\mu_m = \mu_0 (m + 1), \qquad \mu_0 = \frac{d_0}{8 \omega} \approx \frac{1}{16} (2\omega - \beta N N_\nu). \tag{31}$$

Substitution of eq.(30) in the relation

$$f_{2,\omega}(S_2, Y) = \Psi(x, Y) \sqrt{\frac{\omega}{2 \langle S_3 \rangle}} \tag{32}$$

leads to $f_{2,\omega}(S_2, Y)$. We emphasize that the solution in eq.(30) is applicable for arbitrary N. The only approximation used is eq.(26) which was used to derive a closed form of eq.(21).

Limit $(Y - Y_0) \to \infty$: As a check, we consider the solution in $Y - Y_0 \to \infty$ limit. In this case, the non-zero contribution comes only from the term $m = 0$ in eq.(30), giving

$$\Psi(x; \infty) \approx C_0 \, e^{-x^2} \, {}_1F_1 \left(-\mu_0, \frac{1}{2}, x^2 \right). \tag{33}$$

Substitution of eq.(33) in eq.(32) gives

$$f_2(S_2; \infty) \approx C_0 \sqrt{\frac{\omega}{2\langle S_3 \rangle}} \, \mathrm{e}^{-\frac{\omega S_2^2}{2\langle S_3 \rangle}} \, {}_1F_1\left(-\frac{\mu_0}{2}, \frac{1}{2}, \frac{\omega S_2^2}{2\langle S_3 \rangle}\right). \tag{34}$$

Further, with $\omega > N^2$, the limit $N \to \infty$ implies $\omega \to \infty$. Using the limiting Gaussian form of a δ-function, we now have

$$f_2(S_2; \infty) \to \delta(S_2) \tag{35}$$

which is consistent with large N-limit of $S_2 \sim 1/N$ in the entangled limit.

Finite $(Y - Y_0)$**:** For a finite N, ω can be chosen large but finite. A smooth transition for finite N can then be seen in terms of the rescaled variable x (eq.(28)) and a rescaled evolution parameter $\Lambda = 8\omega\mu_0(Y - Y_0)$,

$$\Psi(x; Y - Y_0) \approx \mathrm{e}^{-x^2} \sum_{m=0}^{\infty} C_m \, {}_1F_1\left(-\mu_m, \frac{1}{2}, x^2\right) \mathrm{e}^{-m\Lambda} \tag{36}$$

Here, from eq.(31), μ_0 is positive and finite with $\omega > (\beta/2)NN_\nu$ for any arbitrary N.

The unknown constants C_m in the above equation can be determined if the initial distribution $\Psi(x; Y_0)$ is known. Further insight can however be gained directly by using the expansion

$${}_1F_1\left(-\mu_m, \frac{1}{2}, x^2\right) = {}_1F_1\left(-\mu_0, \frac{1}{2}, x^2\right)\left(1 - 2m\mu_0 x^2 + q_{1m} x^4 + O(x^6)\right) \tag{37}$$

with $q_{1m} \equiv \frac{1}{3}m\mu_0(\mu_0(m - 4) - 1)$. Near $x = 0$, eq.(36) can now be rewritten as

$$\Psi(x; Y - Y_0) \approx \Psi(x; \infty) \sum_{m=0}^{\infty} \frac{C_m \mathrm{e}^{-m\Lambda}}{C_0}\left(1 - 2m\mu_0 x^2 + q_{1m} x^4 + O(x^6)\right) \tag{38}$$

For large Λ, only lower m orders contribute to the series for arbitrary x, giving

$$\Psi(x; Y - Y_0) \approx \Psi(x; \infty)\left[1 + \frac{C_1 \mathrm{e}^{-\Lambda}}{C_0}\left(1 - 2\mu_0 x^2 + q_{11} x^4 + O(x^6)\right)\right], \qquad x \sim 0 \tag{39}$$

$$\approx \Psi(x; \infty) + C_1 \, \mathrm{e}^{-x^2} \, {}_1F_1\left(-2\mu_0, \frac{1}{2}, x^2\right) \mathrm{e}^{-\Lambda} \qquad x \text{ arbitrary} \tag{40}$$

13

From eq.(41), the large Λ distribution near $x = 0$ is thus predicted to be analogous to $\Psi(x;\infty)$. For arbitrary x, however, the additional term in eq.(42) perturbs $\Psi(x;\infty)$, changing the distribution parameters slightly while almost retaining its shape; This is also indicated by our numerical analysis discussed in next section.

For any small $\Lambda > 0$, while the factor $e^{-m\Lambda}$ in eq.(36) becomes increasingly small with increasing m, this can be compensated by the large C_m values and can thereby lead to an intermediate state for $\Psi(x;Y)$, although different from the one at $Y = Y_0$ but close to it. Writing $e^{-m\Lambda} \approx 1 - m\Lambda + O(m^2\Lambda^2)$, eq.(36) gives for arbitrary x,

$$\Psi(x; Y - Y_0) \approx \Psi(x,0) - \Lambda\, e^{-x^2} \sum_{m=0}^{\infty} m\, C_m\, {}_1F_1\left(-\mu_m, \frac{1}{2}, x^2\right) \tag{41}$$

For $x \sim 0$, and, with help of eq.(37), the above can be rewritten as

$$\Psi(x; Y - Y_0) \approx \Psi(x,0) - \Lambda\, \Psi(x,\infty) \sum_{m=0}^{\infty} \frac{mC_m}{C_0}\left(1 - 2m\mu_0 x^2 + q_{1m}\, x^4 + O(x^6)\right) \tag{42}$$

The above indicates the distribution near $x \sim 0$ for finite Y as a superposition of the two distributions: the initial one at $Y = Y_0$ and the other as a perturbed distribution at $Y \to \infty$.

The limit $N \to \infty$ makes it necessary to consider the limit $\omega \to \infty$; a better insight in this case can be derived by writing the distribution in terms of S_2 instead of x. Using eq.(36) in eq.(32) and large order approximation of the function ${}_1F_1\left(-\mu_m, \frac{1}{2}, x^2\right)$ (given in *appendix* B)), we have

$$f_{2,\omega}(S_2, Y - Y_0) \approx \frac{2\, e^{-\frac{\omega S_2^2}{4\langle S_3\rangle}}}{\sqrt{\pi\langle S_3\rangle}} \sum_{m=0}^{\infty} \frac{C_m}{(m+1)} \cos\left(\sqrt{\frac{(m+1)\omega^2 S_2^2}{8\langle S_3\rangle}}\right) e^{-8m\omega\mu_0\,(Y-Y_0)}. \tag{43}$$

As clear from the above, for finite $(Y - Y_0) > 0$, the terms with $m > 0$ can then contribute significantly only if $\omega\mu_0(Y - Y_0) \ll 1$ or the coefficients C_m in eq.(30) are exponentially large overcoming the decay due to $e^{-8m\,\omega\mu_0\,(Y-Y_0)}$. As a generic initial state can not lead to such coefficients, we have

$$f_{2,\omega}(S_2, Y - Y_0) \approx \frac{2\, C_0}{\sqrt{\pi\langle S_3\rangle}}\, e^{-\frac{\omega S_2^2}{4\langle S_3\rangle}} \cos\left(\sqrt{\frac{\omega^2 S_2^2}{8\langle S_3\rangle}}\right). \tag{44}$$

14

The above suggests an abrupt transition, in limit $N \to \infty$, from an initial distribution at $Y - Y_0 = 0$ to the maximum purity for $Y - Y_0 > 0$.

As eq.(30) indicates, a knowledge of the average purity of a typical bipartite eigenstate, in a finite Hilbert space, with corresponding state ensemble given by eq.(6) is not enough; its fluctuations are also important. This can also be seen by a direct calculation of the Y-dependent growth of the variance of purity defined as $\sigma^2(S_2) = \langle \Delta S_2^2 \rangle = \langle (S_2)^2 \rangle - \langle S_2 \rangle^2$ with $\langle (S_2)^n \rangle = \int S_2^n \, f_2(S_2; Y) \, \mathrm{d}S_2$); eq.(21) gives

$$\sigma^2(S_2) \approx \frac{\langle S_3 \rangle}{\omega} - A \, e^{-8\Lambda} \tag{45}$$

with A dependent on the initial state $Y = Y_0$ (details discussed in *appendix* D). Clearly the variance tends to zero for any finite $Y - Y_0$ in limit $\omega, N \to \infty$. The distribution however retains a finite width for finite Λ equivalently finite N as well as $Y - Y_0$.

The relation $R_2 = -\log S_2$ along with eq.(30) can further be used to derive the probability density of second Rényi entropy R_2.

B. Joint Probability Distribution of all moments

For higher order entropies, it is technically easier to first derive the diffusion equation for

$$P_\infty(S_1, S_2, \ldots, S_\infty) = \int \prod_{k=1}^{\infty} \delta(S_k - \sum_n \lambda_n^k) \, P_\lambda \, \mathrm{D}\lambda \tag{46}$$

Following similar steps as in case of S_2 but no longer using any approximation, it can be shown that

$$\frac{\partial P_\infty}{\partial Y} = \sum_{q=1}^{\infty} q \, \frac{\partial}{\partial S_q} \left[\sum_{\substack{t=1 \\ t \neq q}}^{\infty} t \, \frac{\partial}{\partial S_t} S_{q+t-1} + \frac{\partial}{\partial S_q} S_{2q-1} + F(q) \right] P_\infty \tag{47}$$

where $F(q) = 2S_q + (\eta\beta - (q-1))S_{q-1} + \frac{\beta}{2} \sum_{r=0}^{q-1} (S_{q-r-1}S_r - S_{q-1})$.

An integration over undesired variables now leads to the desired distribution. For example, P_q (defined in eq.(15) can also be expressed as

$$P_q = \int P_\infty(S_1, S_2, \ldots, S_\infty) \prod_{t=q+1}^{\infty} \mathrm{d}S_t. \tag{48}$$

The latter expression along with eq.(47) then leads to a diffusion equation for arbitrary q. Eq.(47) also indicates that the lower order moments of the Schmidt eigenvalues and thereby Rényi entropies are dependent on higher order ones. This again indicates that the fluctuations of the entropies can not be ignored.

IV. DISTRIBUTION OF VON NEUMANN ENTROPY

The diffusion equation for the probability density of the Von Neumann entropy, defined in eq.(1) for $\alpha = 1$, can similarly be derived. Using the alternative definition $R_1 = -\sum_{n=1}^{N} \lambda_n \log \lambda_n$, the probability density of R_1 can be written as

$$f_v(R_1; Y) = \int_0^\infty \delta(S_1 - 1) \, P_v(R_1, S_1; Y) \, \mathrm{d}S_1, \tag{49}$$

where $P_v(R_1, S_1; Y)$ is the joint probability density of R_1 and S_1 without the constraint $S_1 = 1$,

$$P_v(R_1, S_1) = \int \delta(R_1 + \sum_n \lambda_n \log \lambda_n) \, \delta(S_1 - \sum_n \lambda_n) \, P_\lambda \, \mathrm{D}\lambda. \tag{50}$$

As in the case of purity, $\delta(S_1 - 1)$ in eq.(49) can again be replaced by its limiting form $g(S_1)$ (eq.(27)), leading to following distribution

$$f_{v,\omega}(R_1; Y) = \int_0^\infty g(S_1) \, P_v(R_1, S_1; Y) \, \mathrm{d}S_1. \tag{51}$$

To proceed further, here again we require a prior knowledge of $\frac{\partial P_v}{\partial Y}$. Differentiating the integral eq. (50) with respect to Y, and using eq.(8) followed by subsequent reduction of the terms by repeated partial integration leads to (see *appendix* A),

$$\begin{aligned}
\frac{\partial P_v}{\partial Y} &= 2\frac{\partial^2}{\partial R_1 \partial S_1} \left[(R_1 - S_1) \, P_v\right] + \frac{\partial^2}{\partial R_1^2} \left[(S_1 - 2R_1)P_v + \langle T_1 \rangle P_v\right] + \frac{\partial^2}{\partial S_1^2}(S_1 \, P_v) \\
&+ \frac{\partial}{\partial R_1} \left[\left(\beta N(N + \nu - 1) + 2\gamma(R_1 - S_1) - \beta\frac{N_\nu}{2}\langle R_0 \rangle + N\right) P_v\right] \\
&+ \frac{\partial}{\partial S_1} \left[\left(2\,\gamma\,S_1 - \frac{1}{2}\beta N N_\nu\right) P_v\right]
\end{aligned} \tag{52}$$

16

with $T_k \equiv \sum_n (\lambda_n)^k (\log \lambda_n)^{k+1}$. Here as discussed in *appendix A*, the above closed form equation for P_v is obtained by using the conditional probability relation $P(R_1, S_1, T_1) = P(T_1|R_1, S_1) \, P_v(R_1, S_1)$ and writing

$$\int T_1 \, P(R_1, S_1, T_1) \, \mathrm{d}T_1 = \langle T_1 \rangle_{R_1, S_1} \, P_v(R_1, S_1). \tag{53}$$

where $\langle T_1 \rangle_{R_1, S_1}$ is the "local average" *i.e.,* ensemble average of T_1 for a given R_1, S_1: $\langle T_1 \rangle_{R_1, S_1} = \int T_1 \, P(T_1|R_1, S_1) \, \mathrm{d}T_1$.

Differentiating eq. (51) with respect to Y and subsequently using eq.(52); a repeated integration by parts along with the relation $f_{v,\omega}(R_1) \to 0$ at the limits $S_1 = 0, \infty$, now leads to following diffusion equation

$$\frac{\partial f_{v,\omega}}{\partial Y} = (t - 2R_1) \frac{\partial^2 f_{v,\omega}}{\partial R_1^2} + (a_1 R_1 + b_1) \frac{\partial f_{v,\omega}}{\partial R_1} + d_0 \, f_{v,\omega}, \tag{54}$$

with,

$$a_1 = 2\gamma + 2\omega \approx 2\omega, \tag{55}$$

$$b_1 = \beta \, (N_\nu - \nu) \, N - \frac{\beta}{2} N_\nu \, \langle R_0 \rangle + N + 2\omega - 2\gamma - 4 + 2\frac{\partial t}{\partial R_1}, \tag{56}$$

$$d_0 = \frac{\beta}{2} \omega \, N \, N_\nu + \omega^2 + (2 - 2\gamma) \, \omega - 2\gamma + \frac{\partial^2 t}{\partial R_1^2}, \tag{57}$$

$$t = 1 + \langle T_1 \rangle_{R_1, S_1 = 1}, \tag{58}$$

$$\langle R_0 \rangle = -\sum_n \langle \log \lambda_n \rangle \approx -N \langle \log \lambda_n \rangle_{e,s} \tag{59}$$

where $N_\nu = N + 2\nu - 1$, and $\langle R_0 \rangle$ implies an ensemble and spectral averaged logarithm of a typical Schmidt eigenvalue (indicated by notation $\langle \rangle_{e,s}$). Here again the above closed form equation is obtained by following approximation

$$\int_0^\infty g(S_1) \, \langle T_1 \rangle_{R_1, S_1} P_2(R_1, S_1; Y) \, \mathrm{d}S_1 \approx \langle T_1 \rangle_{R_1, S_1 = 1}. \tag{60}$$

The above follows by invoking the filtering role of $g(S_1)$; the latter permits approximation of the product term $g(S_1) \, \langle T_1 \rangle_{R_1, S_1}$ by its value at $S_1 = 1$ (the peak of $g(S_1)$). Although here, again, both $\langle T_1 \rangle$ and $\langle R_0 \rangle$ are a function of Y, and consequently the right side of eq.(54) in this case too depends on Y making it technically complicated to solve; nevertheless, both $\langle T_1 \rangle$ and $\langle R_0 \rangle$, changing much slower than R_1, can be assumed almost constant as R_1 evolves

with Y. This permits us to replace $\langle T_1 \rangle_{R_1, S_1=1}$ by its R_1 averaged value $\langle T_1 \rangle$, ignore terms $\frac{\partial t}{\partial R_1}$ and $\frac{\partial^2 t}{\partial R_1^2}$ in eq.(59) and consider a separation of variables approach to solve eq.(54).

Again defining $\Psi_v(x, Y)$ as the transformed probability, given by the relation $f_{v,\omega}(R_1, Y) = \Psi_v(x, Y) \frac{dx}{dR_1}$, the general solution for an arbitrary $Y - Y_0$ can now be given as (*appendix* C),

$$\Psi_v(x; Y - Y_0) \; = \; \frac{1}{2\omega} \left(\frac{4x}{\omega}\right)^\alpha \sum_{m=0}^\infty C_{1m} \; \mathrm{e}^{-m|d_0|(Y-Y_0)} \; {}_1F_1\left(\alpha + \frac{d_m}{2\omega}, \alpha + 1, x\right) \tag{61}$$

with ${}_1F_1(a, b, x)$ as the Kummer's Hypergeometric function [23], $\alpha = \frac{1}{4}(a_1 t + 2b_1 + 4) = \frac{1}{2}(\omega t + b_1)$, $d_m = d_0(m+1)$ and

$$x \equiv -\omega(t - 2R_1) \tag{62}$$

Here, following from the definition in eq.(59), $t \sim 1 + \langle R_1 \rangle^2$.

As in the purity case, here again with $\omega > N^2$ for arbitrary N (with ω large but finite), we can approximate $d_0 \approx \omega^2$ and $b_1 \approx 2\omega$ in eq.(59) (with $\langle R_0 \rangle \sim N \log N + N$ [17]). This in turn gives $\alpha \approx \omega t/2$. Further using the identity ${}_1F_1(a, b; x) = \mathrm{e}^x \, {}_1F_1(b - a, b; -x)$ [23], we can rewrite eq.(61) as

$$\Psi_v(x; Y - Y_0) \; = \; \frac{1}{2\omega} \left(\frac{4x}{\omega}\right)^\alpha \mathrm{e}^x \sum_{m=0}^\infty C_{1m} \; \mathrm{e}^{-m\omega^2(Y-Y_0)} \; \mathcal{F}_M \tag{63}$$

where

$$\mathcal{F}_m \; \equiv \; {}_1F_1\left(1 - \frac{\omega(m+1)}{2}, \frac{\omega t}{2}, -x\right) \approx \mathrm{e}^{\frac{(m+1)x}{t}} \tag{64}$$

and the unknown constant C_{1m} determined by a prior knowledge of $f_v(R_1, Y_0)$. We note that the solution in eq.(61) as well as eq.(63) is applicable for arbitrary N; the only approximation considered here is eq.(B10), used to derive a closed form of eq.(54).

Limit $(Y - Y_0) \to \infty$: In the limit $Y - Y_0 \to \infty$, the non-zero contribution in eq.(63) comes only from the term $m = 0$, giving

$$\Psi_v(x; \infty) \; = \; \frac{C_{10}}{2\omega} \left(\frac{4x}{\omega}\right)^{\omega t/2} \mathrm{e}^x \, \mathcal{F}_0 \tag{65}$$

18

Substitution of eq.(62) in the above equation and using $f_{v,\omega}(x;Y) = 2\omega\Psi_v(x;Y)$, we have

$$f_{v,\omega}(x;\infty) = C_{10} (2R_1 - t)^{\omega t/2} e^{-\omega(t-2R_1)}. \tag{66}$$

Using the limit $f_v(R_1;\infty) = \lim_{\omega\to\infty} f_{v,\omega}(R_1;\infty)$, the above then gives

$$f_v(R_1;\infty) \to \delta(t - 2R_1). \tag{67}$$

Finite $(Y - Y_0)$**:** For finite N, the condition $\omega > N^2$ can be satisfied by a large but finite ω. A smooth crossover from initial distribution at $Y = Y_0$ to that at $Y \to \infty$ can then be seen in terms of the variable x and rescaled evolution parameter $\Lambda = \omega^2(Y - Y_0)$,

$$\Psi_v(x; Y - Y_0) = \frac{1}{2\omega} \left(\frac{4x}{\omega}\right)^{\omega t/2} e^{\frac{x(t+1)}{t}} \sum_{m=0}^{\infty} C_{1m} e^{\frac{m(x-t\Lambda)}{t}} \tag{68}$$

Using $Y = Y_0$ in eq.(63), we have

$$\Psi_v(x; 0) = \frac{1}{2\omega} \left(\frac{4x}{\omega}\right)^{\omega t/2} e^{\frac{x(t+1)}{t}} \sum_{m=0}^{\infty} C_{1m} e^{\frac{mx}{t}}. \tag{69}$$

We note that right side of the above equation is in the form of a discrete Laplace transform; with t large, the sum can be converted into a continuous Laplace transform:

$$\sum_{m=0}^{\infty} C_1(m) e^{\frac{(m+1)x}{t}} = t \int C_1(tz) e^{zx} dz, \tag{70}$$

where $C_1(m) \equiv C_{1m}$. Using the above in eq.(69) gives

$$\int C_1(tz) e^{zx} dz = \frac{2\omega}{t} \left(\frac{\omega}{4x}\right)^{\omega t/2} \Psi_v(x; 0) e^{-x} \tag{71}$$

An inverse transform then gives $C_1(tz)$. Using the relation $C_1(tz) \to C_1(m)$ then lead to the desired coefficients C_{1m}. As can be seen from the above, based on $\Psi_v(x; 0)$ decay for large x, C_{1m} can be large enough to overcome the decaying term $e^{-\frac{m(|x|+t\Lambda)}{t}}$ for small m and Λ. This would result in a deviation of $\Psi_v(x; \Lambda)$ from $\Psi_v(x; 0)$ for finite Λ; it however may just changes the distribution parameters of the initial distribution without significantly affecting its shape. This is also indicated by our numerical analysis discussed in next section.

19

To gain further insights in the behaviour of $\Psi_v(x; Y - Y_0)$, we rewrite eq.(72) as

$$\Psi_v(x; Y - Y_0) \; = \; \Psi_v(x; \infty) \sum_{m=0}^{\infty} \frac{C_{1m}}{C_{10}} \; \mathrm{e}^{\frac{m(x-t\Lambda)}{t}} \tag{72}$$

As $t > 0$, the above indicates a rapid decay of the distribution for large x for arbitrary Λ. For small x too, the distribution stays close to $\Psi_v(x; \infty)$ except for the cases in which the initial distribution $\Psi_v(x; Y_0)$ results in very large C_{1m}. This behaviour is also indicated by our numerical analysis discussed in next section for distribution of R_1.

In limit $N \to \infty$, we need to implement the limit $\omega \to \infty$. As in the purity case, the R_1-distribution can then be better analysed directly from $f_{v,\omega}(R_1; Y | Y_0)$,

$$f_{v,\omega}(R_1; Y | Y_0) \; = \; 2^{\omega t} \; (2R_1 - t)^{\omega t/2} \; \mathrm{e}^{-\frac{\omega(t+1)}{t}(t-2R_1)} \sum_{m=0}^{\infty} C_{1m} \; \mathrm{e}^{-\frac{m\omega}{t}((t-2R_1)+t\omega(Y-Y_0))} \tag{73}$$

As clear from the above, $N \to \infty$ limit again leads to an abrupt transition from an initial distribution at $Y = Y_0$ to $f_v(R_1; Y - Y_0) \to \delta(t - 2R_1)$. If however, for some special initial conditions, C_{1m} values can be large enough to compensate the small values of the factors $\mathrm{e}^{-m\omega^2(Y-Y_0)}$, an intermediate state for $f_v(R_1; Y)$, different from those at $Y = Y_0$ and $Y \to \infty$ may then be reached.

Further insight in the fluctuations of R_1 over the ensemble can be gained by analysing its variance, defined as $\sigma^2(R_1) = \langle \Delta R_1^2 \rangle = \langle (R_1)^2 \rangle - \langle R_1 \rangle^2$ with $\langle (R_1)^n \rangle = \int R_1^n \; f_v(R_1; Y) \; \mathrm{d}R_1$); eq.(54) gives (details discussed in *appendix* E).

$$\sigma^2(R_1) = \frac{1}{a} - B e^{-4\Lambda} \tag{74}$$

The above indicates, as in purity case, a finite width for arbitrary Λ and finite N, and thereby indicating non-negligible fluctuations of R_1 for many body states due to underlying complexity. The limit $N \to \infty$ case however again lead to $P_v(R_1; Y - Y_0)$ approaching a δ function even for finite $Y - Y_0$.

V. NUMERICAL VERIFICATION OF COMPLEXITY PARAMETER BASED FORMULATION OF THE ENTROPIES

Based on the complexity parametric formulation, different reduced matrix ensembles subjected to same global constraints, *e.g.,* symmetry and conservation laws are expected

to undergo similar statistical evolution of the Schmidt eigenvalues. This in turn implies an analogous evolution of their entanglement measures. Intuitively, this suggests the following: the underlying complexity of the system wipes out details of the correlations between two sub-bases, leaving their entanglement to be sensitive only to an average measure of complexity, *i.e.*, $Y - Y_0$. Besides fundamental significance, the complexity parameter based formulation is useful also for the following reason: for states evolving along the same path, Y can be used as a hierarchical criterion even if they belong to different complex systems but subjected to same global constraints.

In a previous work [17], we theoretically predicted that the evolutionary paths for $\langle R_n \rangle$ for different ensembles, with initial condition as a separable state for each of them, are almost analogous in terms of $N^2(Y - Y_0)$. The predictions were numerically verified for three different ensembles of the state matrices C with multi-parametric Gaussian ensemble density. (We recall here that the matrix element C_{kl} of the state matrix C corresponds to a component of a pure state Ψ in product basis $|kl\rangle$ consisting of eigenstate $|k\rangle$ of subsystem A and $|l\rangle$ of subsystem B. A choice of variance of C_{kl} changing with l implies change of correlation between two subunits; this is discussed in detail in [17]. Here the ensembles considered consist of real C matrices with different variance types (with $h_{kl} = \langle C_{kl}^2 \rangle - (\langle C_{kl} \rangle)^2$, $b_{kl} = \langle C_{kl} \rangle$). The study [17] was however based on small-N numerics as well as balanced condition $N_A = N_B = N$ and indicated only an almost collapse onto the same curve in terms of Λ. The investigation was pursued further in the study [21] by a numerical comparison of the dynamics of $\langle R_1 \rangle$ and $\langle R_2 \rangle$ for large size ensembles and for unbalanced condition $N_A \neq N_B$, with $N_A = q^{L_A}$ and q as the size of the local Hilbert space (i.e., the one for a basic unit of which subsystems A and B consist of).

With focus of the present work on the distribution of entanglement entropy, here we consider the same three ensembles to verify the complexity parameter formulation. As discussed in section III.A of [21], it is possible to choose same set of constants $Y_2, \ldots, Y_M$ for BE, PE and EE. The ensembles can briefly be described as follows (details given in [17, 21]):

(i) **Components with same variance along higher columns (BE):** The ensemble parameters in this case are same for all elements of C matrix except those in first column:

$$h_{kl} = \delta_{l1} + \frac{1 - \delta_{l1}}{(1 + \mu)}, \qquad b_{kl;s} = 0, \qquad \forall \ k, l. \tag{75}$$

The substitution of the above in eq.(9) leads to

$$Y = -\frac{N(N_\nu - 1)}{2M\gamma}\left[\ln\left(1 - \frac{2\gamma}{(1+\mu)}\right)\right] + c_0 \tag{76}$$

with constant c_0 determined by the initial state of the ensemble.

Choosing initial condition with $\mu \to \infty$ corresponds to an ensemble of C-matrices with only first column elements as non-zero; this in turn gives $Y_0 = c_0$.

(ii) **Components with variance decaying as a Power law along columns (PE)**: The variance of the matrix elements C_{kl} now changes, as a power law, across the column as well as row but its mean is kept zero:

$$h_{kl} = \frac{1}{1 + \frac{k}{b}\frac{(l-1)}{a}}, \qquad b_{kl} = 0 \quad \forall \ k, l \tag{77}$$

where a and b are arbitrary parameters. Eq.(9) then gives

$$Y = -\frac{1}{2M\gamma}\sum_{r_1=1}^{N}\sum_{r_2=1}^{N_\nu - 1}\ln\left(1 - \frac{2\gamma}{1 + \frac{r_1}{a}\frac{r_2}{b}}\right) + c_0 \tag{78}$$

Choosing initial condition with $b, a \to \infty$ again corresponds to an ensemble of C-matrices with only first column elements as non-zero and thereby $Y_0 = c_0$.

(iii) **Components with variance exponentially decaying along columns (EE)**: Here again the mean is kept zero for all elements but the variance changes exponentially across the column as well as row of C-matrix:

$$h_{kl} = \exp\left(-\frac{k|l-1|}{ab}\right), \qquad b_{kl} = 0 \qquad \forall \ k, l \tag{79}$$

with b as an arbitrary parameter. Eq.(9) now gives

$$Y = -\frac{1}{2M\gamma}\sum_{r_1=1}^{N}\sum_{r_2=1}^{N_\nu - 1}\ln\left(1 - \frac{2\gamma}{\exp(\frac{r_1}{a}\frac{r_2}{b})}\right) + c_0 \tag{80}$$

with $M = NN_\nu$. Here again the initial choice of parameters $b, a \to \infty$ leads to a C-matrix ensemble same as in above two cases and same Y_0.

As discussed in [17, 21], the change of variance along the columns, in each of the three ensembles described above, ensures a variation of average entanglement entropy from an initial separable state to maximally entangled state. Here the separable state corresponds

to $\mu \to \infty$ for BE and $a \to 0, b \to 0$ (equivalently $Y \to Y_0$) for PE and EE. The maximally entangled state corresponds to $\mu \to 0$ for BE and very large a, b for PE and EE.

For numerical analysis of various entropies, we exactly diagonalize each matrix of the ensembles with a fixed matrix size, and for many values of the ensemble parameters a, b but with fixed $\gamma = 1/4$. For simplification, we consider a balanced bipartition, such that the C matrix chosen for all cases is a $N \times N$ square matrix. The obtained Schmidt eigenvalues are then used to obtain R_1 and S_2 for each matrix. Repeating the procedure for each matrix of the ensemble, we obtain a distribution of R_1 and S_2 over the ensemble for a specific Y value. (The latter corresponds to a set of ensemble parameters for a given ensemble and can be obtained for BE, PE and EE from eq.(76), eq.(78) and eq.(80) respectively. To study its Y-dependence, we numerically derive the distribution for many Y-values. As in previous studies [17, 21], here again we assume the basic units as the qubits, thus implying $q = 2$.

Figures 1-3 depict the distributions of purity for BE, PE and EE respectively, each case considered at six different Y-values. From eqs.(76, 78, 80), a same Y value for the three ensembles requires consideration of different combinations of ensemble parameters. As figures indicates, the initial distribution (for $Y = Y_0 = 10^{-5}$) is well-described by the *Log-Gamma* behaviour ($f(r, c) = \frac{\exp(cr - e^r)}{\Gamma(c)}$) with $r = \frac{(S_2 - loc)}{scale}$. The crossover behaviour for small $Y - Y_0$ is well-fitted by the *Log-Gamma* behaviour but the distribution parameters change (given in table I): this is consistent with our theoretical prediction for purity case given by eqs.(41, 42).

For $Y - Y_0 \sim 1/N$ (i.e $Y \sim 10^{-3}$ with $N = 1024$) , however, the form of the distribution changes from *Log-Gamma* to *Beta* distribution ($f(r, a, b) = \frac{\Gamma(a+b)}{\Gamma(a)\Gamma(b)} r^{a-1}(1 - r)^{b-1}$). As predicted by eq.(38), the large $Y - Y_0$ limit finally converges to a narrow width *Gaussian* ($f(r, \sigma^2) = \frac{\exp(-r^2/2\sigma^2)}{\sqrt{2\pi\sigma^2}}$). The details of the fitted parameters i.e *loc*, *scale* and *c* for each distribution are given in table I. As the latter indicates, the location parameter *loc* for different Y varies significantly. For comparison of the distribution for different Y values, we have shifted each distribution by corresponding *loc* values; this ensures same centring for them. It is worth noting from table I that the shape of the S_2-distribution remains analogous for BE, PE and EE for a given Y although their stability parameters are different. An analogy of shape for a given Y verifies our theoretical prediction that the distribution of purity for the ensembles represented by eq.(6) is governed not by individual parametric details of the ensemble but by complexity parameter Y. Due to different stability parameters

for initial S_2-distribution of BE, PE and EE, a difference in their stability parameters for $Y > Y_0$ is also consistent with our formulation.

Figures 4-6 displays the distributions of von Neumann entropies (corresponding to each purity case depicted in Figures 1-3). The initial distribution at $Y_0 = 10^{-5}$ is now well-fitted by the *Gamma* behaviour ($f(r,a) = \frac{r^{a-1} e^{-r}}{\Gamma(a)}$) with $r = (R_1 - loc) / scale$. As predicted by our theory, the behaviour during crossover varies from *Gamma* distribution to *Log-Gamma* and finally ending in a narrow Gaussian (near $Y \sim 1$); the fitted distribution parameters for each case are given in table II. In contrast to purity, the shape of the R_1-distribution changes from *Gamma* to *Log-Gamma* at $Y \sim 1/N$ (with $N = 1024$). But as can be seen from the table II, for a given Y, the shape remains analogous for BE, PE and EE although the distribution parameters are again different.

As clear from each of the figures, the distribution of both entropies approach a narrow distribution for small Y ($\sim 10^{-5}$) and large $Y \geq 1$, respectively. For intermediate Y values ($Y \sim \frac{1}{N}$), however, the distributions have non-zero finite width. This indicates the following: as both entropies involve a sum over functions of the Schmidt eigenvalues, their local fluctuations are averaged out in separable and maximally entangled limit. For the partial entanglement region, corresponding to finite non-zero Y (specifically, where average entropy changes from linear Y-dependence to a constant in Y), the eigenvalue fluctuations are too strong to be wiped out by summation, resulting in significant fluctuations of the entropies. Indeed $Y \sim \frac{1}{N}$ marks the edge between separability and fully entangled limit of the state: states are fully separable for $Y < 1/N$ and fully entangled for $Y > 1/N$. As indicated in [17, 21], many average measures of Schmidt eigenvalues undergo a rapid change from one constant value to another in the vicinity of $Y \sim \frac{1}{N}$.

It is also worth noting that the distribution for $Y \sim 1$ is almost same for all three cases; this suggests that the distributions are almost independent of ensemble details *i.e.,* local constraints and reach ergodic limit as $Y \sim 1$ is reached. Further, the finite width of the distributions also indicate that, for finite N, the fluctuations of S_2 and R_1 around their average can not be neglected; this has implications for ordering the states in increasing entanglement using purity or von Neumann entropy as the criteria. We also find that the distributions are dependent on the ratio of subsystem sizes N_A/N_B; (the figures included here correspond to $N_A = N_B$ only).

Figure 7 also displays the Y governed evolution of the standard deviations $\sigma(S_2), \sigma(R_1)$

of S_2 and R_1-distributions. The collapse of the curves depicting $S_2(Y)$ behaviour for BE, PE, EE for entire Y range, from separability to maximum entanglement, to same curve is consistent with our single parametric formulation of the fluctuations of entanglement measures for pure states described by eq.(6). This is reconfirmed by a similar collapse for R_1. As can also be seen from the figure, although the standard deviation of entanglement measures in the separable and maximally entangled regimes is vanishing, as $N \to \infty$, in the intermediate regime the fluctuations are orders of magnitude larger. Observation of such trends in quantum fluctuation measures are believed to indicate a quantum phase transition [24, 25] and the idea has already been used to study thermalization $\to$ many-body localization transition in disordered systems [26]. This indeed lends credence to the state matrix models used in our analysis: although mimicking underlying complexity of the state through Gaussian randomness, they turn out to be good enough to capture interesting many-body phenomena.

We note, while a lack of closed form formulation of the distributions (i.e eq.(33) and eq.(72)) for finite N makes it technically challenging to express their parameters as a function of $Y - Y_0$ and compare with our numerical results, an analogous shape for a given Y and the change with increasing Y is consistent with our theoretical prediction. This can also be seen from table I. and II: the form of the distributions for each Y is analogous for BE, PE and EE although their distribution parameters are different. The latter is expected as the initial conditions chosen in numerics for each ensemble are different.
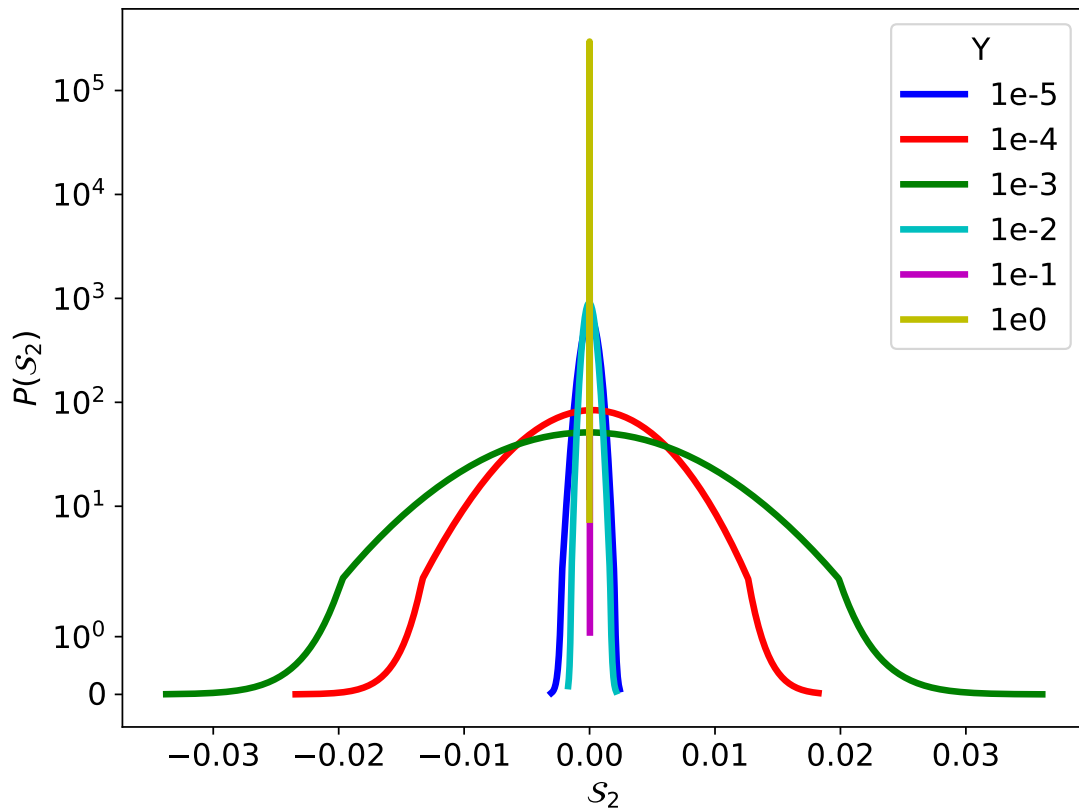
FIG. 1. **Distribution of purity for the Brownian state ensemble (BE, eq.(75)):** The figure displays the distribution of the purity $\mathcal{S}_2 \equiv S_2 - \langle S_2 \rangle$ for different Y-values, ranging from almost separable limit to maximally entangled regimes over BE consisting of 10^5 square C-matrices each of size $N = 1024$. Here, to compare the distributions for different Y. S_2 is shifted by $\langle S_2 \rangle$ (the ensemble average for a fixed Y). With Y increasing, numerically obtained distribution changes from an initial *Log-normal* form (at $Y = 10^{-5}$) to *Beta* and finally to *Normal* distribution (for $Y \sim 1$). To take into account rapidly diverging distributions with increasing Y, a symmetric log scale is used for $y-$ axis. The goodness of fit for each distribution has been tested by minimizing the residual sum of squares (RSS) [27]; details about the best fit distribution are given in table I.
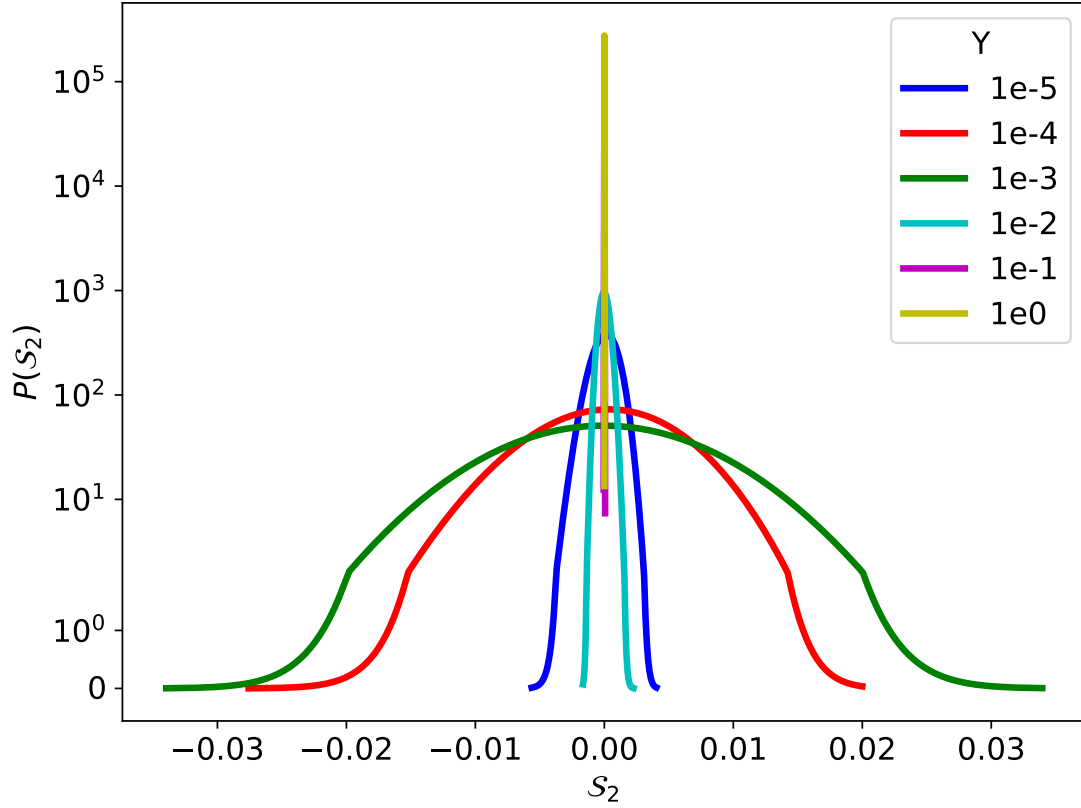
FIG. 2. **Distribution of purity for power-law state ensemble (PE):** The details here are same as in figure 1, except now the ensemble concerned is described by eq.(77). Here again an increasing Y leads to a crossover of the numerically derived distribution from an initial *Log-normal* form (at $Y = 10^{-5}$) to *Beta* and finally to *Normal* distribution (for $Y \sim 1$). We note that the shape for each Y is analogous to those in BE cases although best fit parameters (table I) are different; this is consistent our theory.
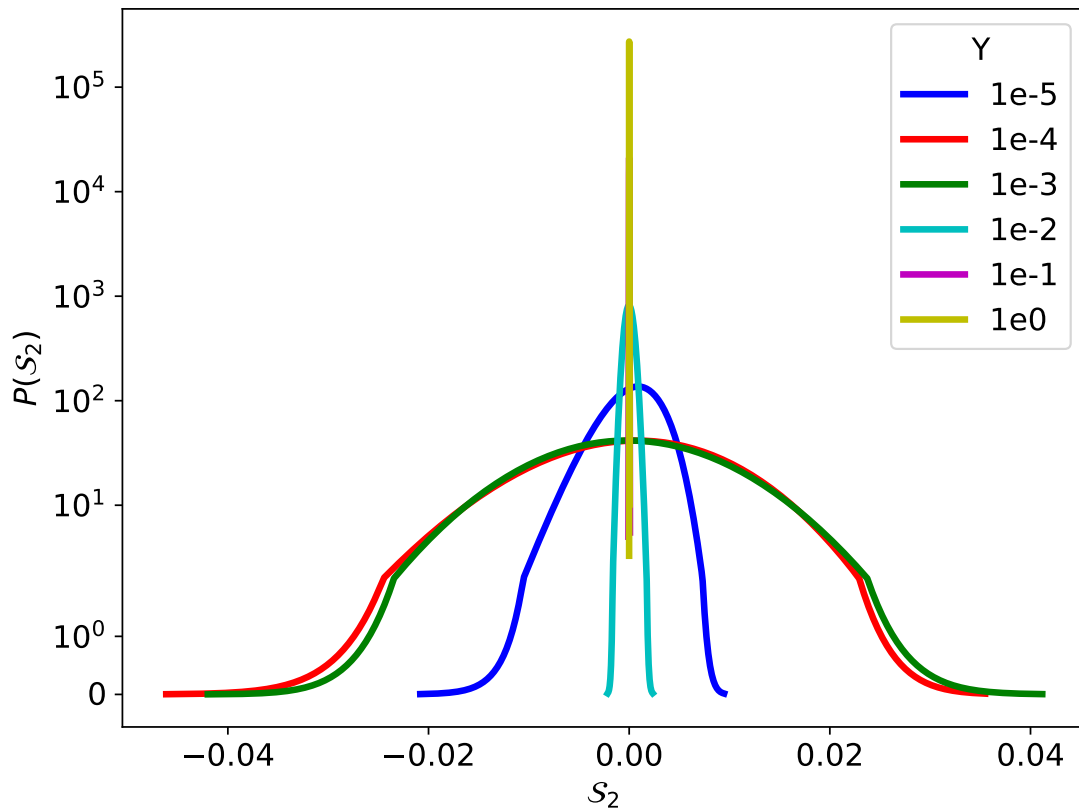
FIG. 3. **Distribution of purity for exponential state ensemble (EE):** The details here are same as in figures 1 and 2, except now the ensemble concerned is described by eq.(79). In analogy with BE and PE cases, an increasing Y again leads to a change of the distribution from an initial *Log-normal* form (at $Y = 10^{-5}$) to *Beta* and finally to *Normal* distribution (for $Y \sim 1$). Consistent with our theory, here too the shape for each Y is similar to those in BE and PE cases although best fit parameters (table I) vary.
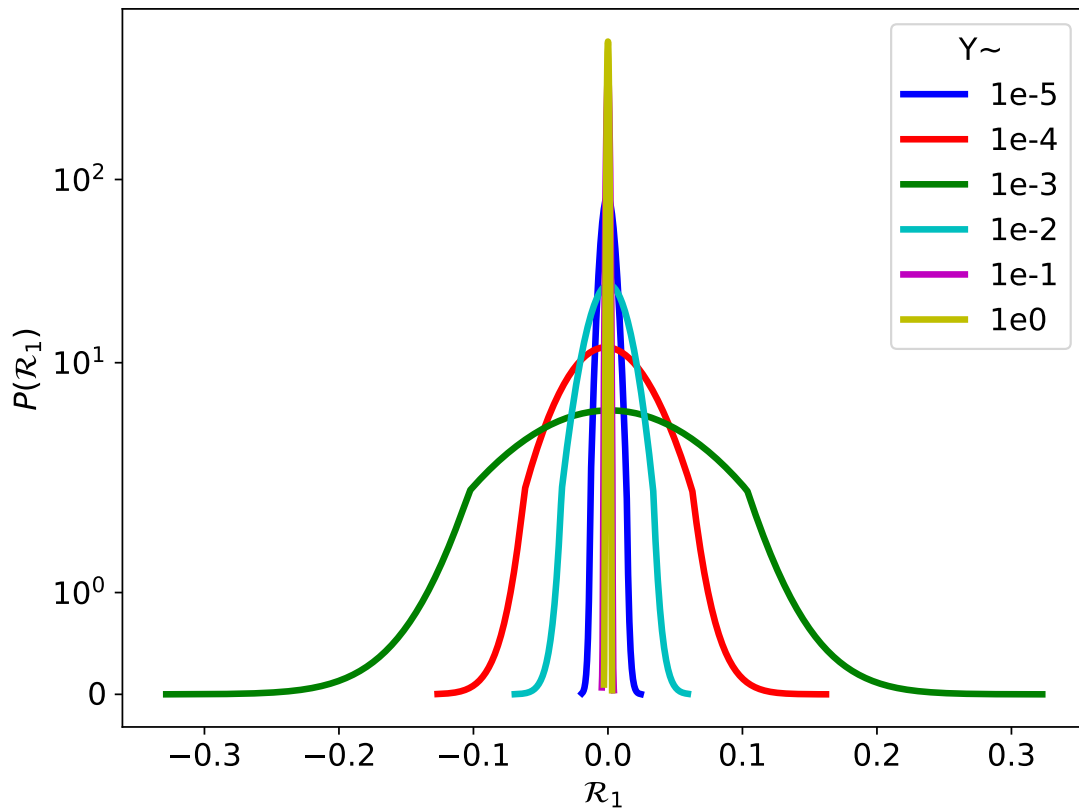
FIG. 4. **Distribution of von Neumann entropy for Brownian state ensemble (BE, eq.(75)):** The details here are same as in figure 1, except now the entanglement measure considered here is the von Neumann entropy $\mathcal{R}_1 \equiv R_1 - \langle R_1 \rangle$ with $\langle R_1 \rangle$ implying an ensemble average of R_1 for a fixed $Y - Y_0$. The shape of the numerically obtained distribution now changes from *Gamma* to *Log-Gamma* to *Normal* for each Y, with best fit parameters for each case are given in table I.
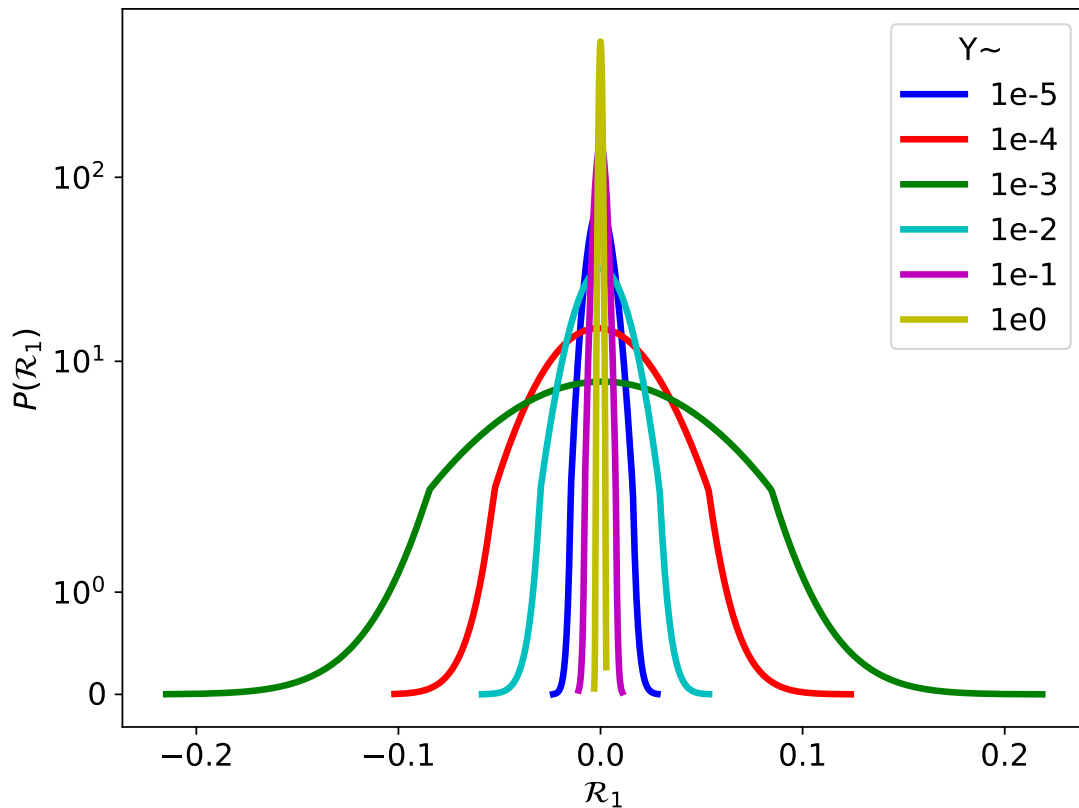
FIG. 5. **Distribution of von Neumann entropy for power-law state ensemble (PE, eq.(77)):** The details here are same as in figure 2, except now the measure considered here is von Neumann entropy $\mathcal{R}_1 \equiv R_1 - \langle R_1 \rangle$ with $\langle R_1 \rangle$ implying an ensemble average of R_1 for a fixed $Y - Y_0$. Analogous to BE case, the shape of the numerically obtained distribution changes from *Gamma* to *Log-Gamma* to *Normal* for each Y, with best fit parameters given in table II.
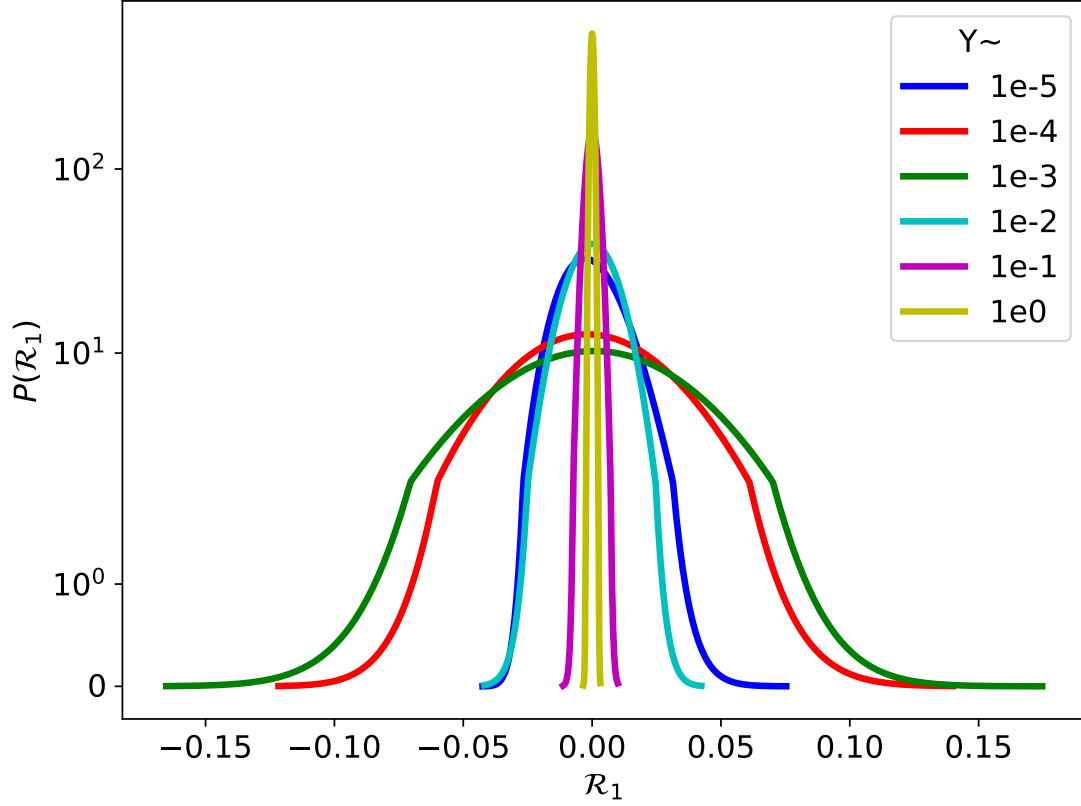
FIG. 6. **Distribution of von Neumann entropy for exponential state ensemble (EE, eq.(79)):** The details here are same as in figure 3, except now the measure considered here is von Neumann entropy $\mathcal{R}_1 \equiv R_1 - \langle R_1 \rangle$ with $\langle R_1 \rangle$ implying an ensemble average of R_1 for a fixed $Y - Y_0$. Similar to BE and PE cases, an increasing Y again leads to a change of the numerically derived distribution from an initial *Gamma* form (at $Y = 10^{-5}$) to *Log-Gamma* and finally to *Normal* distribution (for $Y \sim 1$). Consistent with our theory, here too the shape for each Y is similar to those in BE and PE cases although best fit parameters (table I) vary.
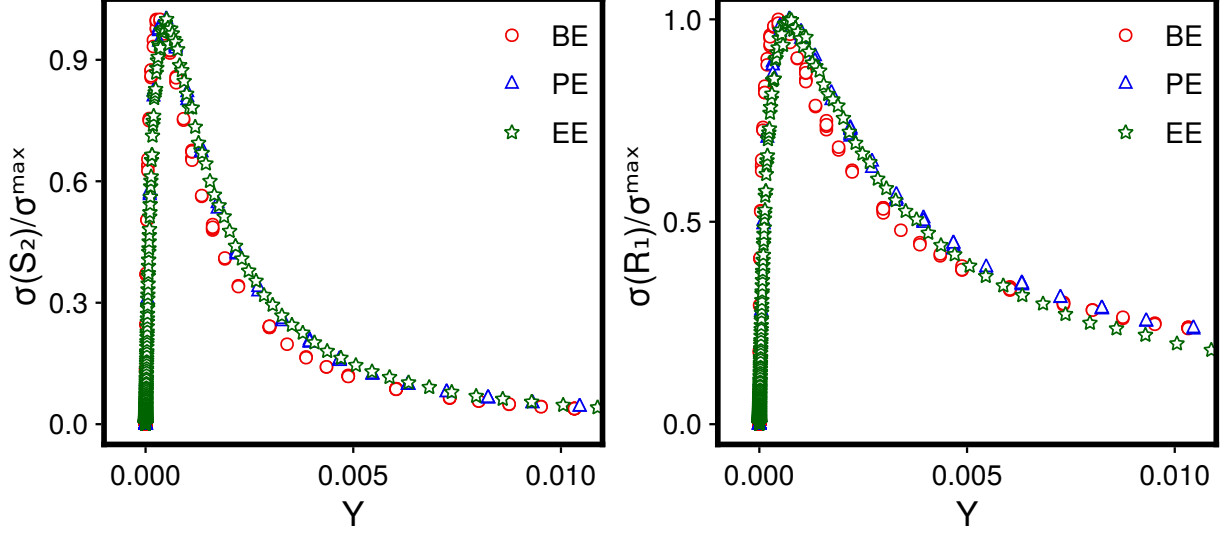
FIG. 7. **Parametric evolution of the standard deviation of purity and entanglement entropy:** The figure displays the evolution of the standard deviation $\sigma(S_2)$ of the purity and $\sigma(R_1)$ of von Neumann entropy (measured in units of σ_{max}) for BE, PE and EE, defined in eq.(75), eq.(77) and eq.(79), as the complexity parameter Y varies from separability to maximum entanglement limit. Each ensemble used consists of 5000 matrices of size $N = 1024$. Here σ_{max} refers to the maximum standard deviation reached for an ensemble during Y governed evolution. The collapse of the behaviour for different ensembles to same curve signifies the universality of the Y governed evolution of the standard deviation. As can be seen from both parts, a spike occurs at $Y \sim 1/N$; this indicates a transition from a separable to maximum entanglement regime at $Y \sim 1/N$. Such pattern is usually observed when the system goes under a quantum phase transition, *e.g.,* thermalization to localization transition.

TABLE I. **Details of the fitted distributions for S_2 in figures 1-3 :** The parameters for the Log-Gamma distribution $f(r,c) = \frac{\exp(cr - e^r)}{\Gamma(c)}$ (labeled as L-Gamma), Beta distribution, $f(r,u,v) = \frac{\Gamma(u+v)\, r^{u-1}(1-r)^{v-1}}{\Gamma(u)\Gamma(v)}$ and Gaussian distribution $f(r) = \frac{\exp(-r^2/2)}{\sqrt{2\pi}}$ with $r \equiv \frac{(S_2 - loc)}{scale}$.

Y	10^{-5}	10^{-4}	10^{-3}	10^{-2}	10^{-1}	1
BE, μ	100989.553	10013.156	1009.816	98.622	8.843	0.276
Function	L-Gamma	L-Gamma	Beta	Beta	Beta	Normal
LOC	0.960	0.542	0.194	0.006483	0.00196	0.00195
Scale	0.0047	0.057	0.123	0.013	122.152	1.36e-06
c	59.747	140.296	-	-	-	-
u	-	-	26.998	38.163	129.888	-
v	-	-	34.981	114.458	2.615e+08	-
PE, (a,b)	(1.399, 0.175)	(11.1969, 0.174)	(4.723, 4.723)	(232.862, 1.399)	(302.318, 21.869)	(859.542, 859.542)
Function	L-Gamma	L-Gamma	Beta	Beta	Beta	Normal
LOC	0.961	0.659	-34.122	0.0157	0.0044	0.00199
Scale	0.0044	0.041	40.859	0.014	0.000197	1.454e-06
c	18.039	56.205	-	-	-	-
u	-	-	3.069e+06	69.694	21.887	-
v	-	-	578418	164.73	23.402	-
EE, (a,b)	(21.869, 0.1749)	(127.540, 0.175)	(859.542, 0.175)	(302.318, 4.723)	(859.542, 21.869)	(1020.323, 859.542)
Function	L-Gamma	L-Gamma	Beta	Beta	Beta	Normal
LOC	0.983	0.604	0.249	0.0313	0.0067	0.002
Scale	0.00429	0.0657	0.169	298.225	4.331	1.466e-06
c	2.34	48.119	-	-	-	-
u	-	-	33.613	259.605	394.349	-
v	-	-	43.65	9.727e+06	4.516e+06	-

TABLE II. **Details of the fitted distributions for R_1 in figures 4-6 :** The parameters for the Log-Gamma distribution $f(x,c) = \frac{\exp(cr-e^r)}{\Gamma(c)}$ (labelled as L-Gamma), Gamma distribution $f(r,v) = \frac{r^{v-1}e^{-r}}{\Gamma(v)}$ and Gaussian distribution $f(r) = \frac{\exp(-r^2/2)}{\sqrt{2\pi}}$ with $r \equiv \frac{(R_1-loc)}{scale}$.

Y	10^{-5}	10^{-4}	10^{-3}	10^{-2}	10^{-1}	1
BE, μ	100989.553	10013.156	1009.816	98.622	8.843	0.276
Function	Gamma	Gamma	L-Gamma	L-Gamma	L-Gamma	Gaussian
LOC	0.093	0.509	-5.122	8.405	9.218	9.279
Scale	0.000299	0.0014	1.702	0.116	0.01	0.00071
c	-	-	564.835	60.837	89.027	-
v	270.677	568.46	-	-	-	-
PE, (a,b)	(1.399, 0.175)	(11.1969, 0.174)	(4.723, 4.723)	(232.862, 1.399)	(302.318, 21.869)	(859.542, 859.542)
Function	Gamma	Gamma	L-Gamma	L-Gamma	L-Gamma	Gaussian
LOC	0.0963	0.45	-7.05	4.992	7.9197	9.26
Scale	0.00039	1.634	1.6337	0.323	0.0759	0.00073
c	-	-	1018.62	673.32	861.339	-
v	210.84	454.897	-	-	-	-
EE, (a,b)	(21.869, 0.1749)	(127.540, 0.175)	(859.542, 0.175)	(302.318, 4.723)	(859.542, 21.869)	(1020.323, 859.542)
Function	Gamma	Gamma	L-Gamma	L-Gamma	L-Gamma	Gaussian
LOC	0.022	-0.023	-4.5443	3.056	7.395	9.255
Scale	0.0031	0.0016	1.08677	0.32	0.032	0.00074
c	-	-	796.975	1017.28	171.335	-
v	16.628	370.069	-	-	-	-

VI. CONCLUSION

In the end, we summarize with a brief discussion of our main idea, results, and open questions. We have theoretically analysed the distribution of entanglement measures of a typical quantum state in a bipartite basis. While previous theoretical studies have mostly considered ergodic states, leading to a standard Wishart ensemble representation of the reduced density matrix, our primary focus in this work has been on the non-ergodic states, specifically, the states with their components (in bipartite basis) Gaussian distributed with arbitrary mean and variances, subjected to symmetry constraints, in addition. This in turn gives the reduced density matrix as a multi-parametric Wishart ensemble with fixed trace and permits an analysis of the entanglement with changing system conditions, *i.e.,* complexity of the system. Our approach is based on the complexity parameter formulation of the joint probability distribution of the Schmidt eigenvalues which in turn leads to the evolution

equations for the distributions of the Rényi and von Neumann entropies. As clearly indicated by the theoretical formulations for the probability densities for finite Y, reconfirmed by numerical analysis of the distributions and their standard deviation, a knowledge of the average entanglement measures is not sufficient for complex systems, their fluctuations are indeed significant, and any hierarchical arrangement of states based solely on the averages may lead to erroneous results.

The complexity parameter based formulation of the entanglement distributions discussed here has many potential applications. For example, the current quantum purification schemes for communication through noisy quantum channels are based on distillation of entanglement in the ensemble i.e by increasing the entropy for a part of the ensemble at the cost of the other part. In contrast, our formulation is based on an evolution of the entropy of a typical quantum state in the ensemble to its maximum value.

Another potential use of our formulation is to identify various classes of quantum states with same entanglement entropy; this follows as the entanglement entropy for each class is characterized by the complexity parameter Y (besides constants of evolution). For example, consider the states belonging to two different ensembles, characterized by sets $\{h, b\}$ and $\{\tilde{h}, \tilde{b}\}$; (different ensembles here may refer e.g. different origins of the states). If however both ensembles correspond to same value of the complexity parameter as well as constant of evolution, the distribution of their entanglement entropies over respective ensembles are predicted to be same.

As an increasing Y results in an increase in entanglement entropy, maximum entanglement for a class of quantum states can be achieved by controlling Y only without considering specific details of the ensemble parameters. The information can also be used for a hierarchical arrangement of partially entangled states (*e.g.,* revealing the flaws in their characterization based on average behaviour) as well as for phase transition studies of many body systems.

The present study still leaves many open questions. For example, a typical many-body state of a quantum system may be subjected to additional constraints and need not be represented by a multiparametric Wishart ensemble with fixed trace only. It is then natural to query about the role of additional constraints on the growth of entanglement measure. The question is relevant in view of the recent studies indicating different time-dependent growth rates in constrained systems [28, 29]. A generalization of the present results to bipartite mixed states as well as multipartite states is also very much desirable and will be

presented in near future.

Another question is regarding the explicit role played by the system parameters in the entanglement evolution. The complexity parameter depends on the system parameters through distribution parameters. A knowledge of their exact relation, however, requires a prior knowledge of the quantum Hamiltonian, its matrix representation in the product basis as well as the nature and distribution parameters of the appropriate ensemble. The knowledge leads to the determination of the appropriate ensemble of its eigenstates. A complexity parameter formulation for the Hermitian operators, *e.g.,* many-body Hamiltonians, and their eigenstates has already been derived. As the evolution equation of the JPDF of the components of an eigenfunction can in principle be derived from that of the ensemble density of the Hamiltonian, the evolution parameter of the former must be dependent on the latter. This work in currently in progress.

ACKNOWLEDGMENTS

[1] W. Dür and H. J. Briegel, "Entanglement purification and quantum error correction," *Reports on Progress in Physics*, vol. 70, no. 8, p. 1381, 2007.

[2] C. H. Bennett, D. P. DiVincenzo, J. A. Smolin, and W. K. Wootters, "Mixed-state entanglement and quantum error correction," *Physical Review A*, vol. 54, no. 5, p. 3824, 1996.

[3] E. P. Wigner, "Random matrices in physics," *SIAM review*, vol. 9, no. 1, pp. 1–23, 1967.

[4] D. N. Page, "Average entropy of a subsystem," *Physical Review Letters*, vol. 71, no. 9, p. 1291, 1993.

[5] E. Bianchi, L. Hackl, M. Kieburg, M. Rigol, and L. Vidmar, "Volume-law entanglement entropy of typical pure quantum states," *PRX Quantum*, vol. 3, no. 3, p. 030201, 2022.

[6] S. N. Majumdar, "Extreme eigenvalues of wishart matrices: application to entangled bipartite system," *arXiv preprint arXiv:1005.4515*, 2010.

[7] S. Kumar and A. Pandey, "Entanglement in random pure states: spectral density and average von neumann entropy," *Journal of Physics A: Mathematical and Theoretical*, vol. 44, no. 44, p. 445301, 2011.

[8] C. Nadal, S. N. Majumdar, and M. Vergassola, "Statistical distribution of quantum entanglement for a random bipartite state," *Journal of Statistical Physics*, vol. 142, pp. 403–438, 2011.

[9] P. Vivo, M. P. Pato, and G. Oshanin, "Random pure states: Quantifying bipartite entanglement beyond the linear statistics," *Physical Review E*, vol. 93, no. 5, p. 052106, 2016.

[10] M. J. Hall, "Random quantum correlations and density operator distributions," *Physics Letters A*, vol. 242, no. 3, pp. 123–129, 1998.

[11] O. Giraud, "Purity distribution for bipartite random pure states," *Journal of Physics A: Mathematical and Theoretical*, vol. 40, no. 49, p. F1053, 2007.

[12] L. Wei, "Skewness of von neumann entanglement entropy," *Journal of Physics A: Mathematical and Theoretical*, vol. 53, no. 7, p. 075302, 2020.

[13] S.-H. Li and L. Wei, "Moments of quantum purity and biorthogonal polynomial recurrence," *Journal of Physics A: Mathematical and Theoretical*, vol. 54, no. 44, p. 445204, 2021.

[14] Y. Huang, L. Wei, and B. Collaku, "Kurtosis of von neumann entanglement entropy," *Journal of Physics A: Mathematical and Theoretical*, vol. 54, no. 50, p. 504003, 2021.

[15] D. J. Luitz, "Long tail distributions near the many-body localization transition," *Phys. Rev. B*, vol. 93, p. 134201, Apr 2016.

[16] P. Shukla, "Eigenfunction statistics of wishart brownian ensembles," *Journal of Physics A: Mathematical and Theoretical*, vol. 50, p. 435003, oct 2017.

[17] D. Shekhar and P. Shukla, "Entanglement dynamics of multi-parametric random states: a single parametric formulation," *Journal of Physics A: Mathematical and Theoretical*, vol. 56, p. 265303, jun 2023.

[18] P. Shukla, "Level statistics of anderson model of disordered systems: connection to brownian ensembles," *Journal of Physics: Condensed Matter*, vol. 17, no. 10, p. 1653, 2005.

[19] T. Mondal and P. Shukla, "Spectral statistics of multiparametric gaussian ensembles with chiral symmetry," *Phys. Rev. E*, vol. 102, p. 032131, Sep 2020.

[20] P. Shukla, "Alternative technique for complex spectra analysis," *Physical Review E*, vol. 62, no. 2, p. 2098, 2000.

[21] D. Shekhar and P. Shukla, "Edge of entanglement in non-ergodic states: a complexity parameter formulation," *arxiv.org//arXiv.2310.12796*, 2023.

[22] S. Bera and A. Lakshminarayan, "Local entanglement structure across a many-body localization transition," *Physical Review B*, vol. 93, 4 2016.

[23] F. W. J. Olver, A. B. O. Daalhuis, D. W. Lozier, B. I. Schneider, R. F. Boisvert, C. W. Clark, B. V. S. B. R. Mille and, H. S. Cohl, and e. M. A. McClain, "Nist digital library of mathematical functions." http://dlmf.nist.gov/, Release 1.0.26 of 2020-03-15, 2020.

[24] G. Vidal, J. I. Latorre, E. Rico, and A. Kitaev, "Entanglement in quantum critical phenomena," *Phys. Rev. Lett.*, vol. 90, p. 227902, Jun 2003.

[25] T. J. Osborne and M. A. Nielsen, "Entanglement in a simple quantum phase transition," *Phys. Rev. A*, vol. 66, p. 032110, Sep 2002.

[26] D. J. Luitz, N. Laflorencie, and F. Alet, "Many-body localization edge in the random-field heisenberg chain," *Physical Review B*, vol. 91, p. 081103, 2 2015.

[27] E. Taskesen, "distfit is a python library for probability density fitting.," Jan. 2020.

[28] T. Zhou and A. W. W. Ludwig, "Diffusive scaling of rényi entanglement entropy," *Phys. Rev. Res.*, vol. 2, p. 033020, Jul 2020.

[29] T. Rakovszky, F. Pollmann, and C. W. von Keyserlingk, "Sub-ballistic growth of rényi entropies due to diffusion," *Phys. Rev. Lett.*, vol. 122, p. 250602, Jun 2019.

Appendix A: Derivation of eqs. (19) and (52)

From the definition in eq.(15), we have for $k = 2$, the JPDF P_2 of S_2 and S_1.

For $X(\lambda)$ as an arbitrary function of eigenvalues $\lambda_1 \ldots \lambda_N$, the JPDF P_x of S_1 and $X(\lambda)$ can be defined as

$$P_x(S_1, X; Y) = \int \delta_1 \, \delta_x \, P_\lambda(\lambda; Y) \, \mathrm{D}\lambda, \tag{A1}$$

with $\delta_x \equiv \delta(X - X(\lambda)$ and δ_1 defined below eq.(15) and $P_\lambda(\lambda) \to 0$ at the two integration limits $0 \le \lambda_n \le \infty \; \forall n = 1 \cdots N$. We note here that the constraint δ_1 effectively reduces the limits to $\frac{1}{N} \le \lambda_n \le 1$.

A differentiation of the above equation with respect to Y and subsequently using eq.(A1) gives

$$\frac{\partial P_x(S_1, X; Y)}{\partial Y} = \int \delta_1 \, \delta_x \, \frac{\partial P_\lambda}{\partial Y} \, \mathrm{D}\lambda = I_1 + I_2, \tag{A2}$$

with I_1 as,

$$I_1 = -C_{hs} \sum_{n=1}^{N} \int_0^\infty \delta_1 \, \delta_x \, \frac{\partial}{\partial \lambda_n} \left(\sum_{m=1}^{N} \frac{\beta \lambda_n}{\lambda_n - \lambda_m} + \beta \nu - 2\gamma \lambda_n \right) P_\lambda \, \mathrm{D}\lambda, \tag{A3}$$

and,

$$I_2 = C_{hs} \sum_{n=1}^{N} \int \delta_1 \, \delta_x \, \frac{\partial^2 (\lambda_n \, P_\lambda)}{\partial \lambda_n^2} \, \mathrm{D}\lambda. \tag{A4}$$

Integration by parts, and, subsequently using the relation $P_\lambda(\lambda) \to 0$ at the integration limits, now gives

$$I_1 = C_{hs} \sum_{n=1}^{N} \int_0^\infty \left[\frac{\partial \delta_1}{\partial \lambda_n} \delta_x + \delta_1 \frac{\partial \delta_x}{\partial \lambda_n} \right] \left(\sum_{m=1}^{N} \frac{\beta \lambda_n}{\lambda_n - \lambda_m} + \beta \nu - 2\gamma \lambda_n \right) P_\lambda \, \mathrm{D}\lambda. \tag{A5}$$

Again using $\frac{\partial \delta_a}{\partial \lambda_n} = -\frac{\partial \delta_a}{\partial a} \frac{\partial a(\lambda)}{\partial \lambda_n}$ with $a = S_1$ or X, I_1 can be rewritten as

$$I_1 = \frac{\partial}{\partial S_1} \left(2\gamma \, S_1 - \frac{1}{2} \beta N(N + 2\nu - 1) \right) P_x + I_0, \tag{A6}$$

where,

$$I_0 = -C_{hs} \frac{\partial}{\partial X} \int \delta_1 \, \delta_x \left[\sum_{n=1}^{N} \frac{\partial X}{\partial \lambda_n} \left(\sum_{m=1}^{N} \frac{\beta \lambda_n}{\lambda_n - \lambda_m} + (\beta \nu - 2\gamma \lambda_n) \right) \right] P_\lambda \, \mathrm{D}\lambda. \tag{A7}$$

Similarly, a repeated partial differentiation gives

$$I_2 = C_{hs} \sum_{n=1}^{N} \int \left[\delta_1 \frac{\partial^2 \delta_x}{\partial \lambda_n^2} + 2 \frac{\partial \delta_1}{\partial \lambda_n} \frac{\partial \delta_x}{\partial \lambda_n} + \frac{\partial^2 \delta_1}{\partial \lambda_n^2} \delta_x \right] \lambda_n P_\lambda \, D\lambda. \tag{A8}$$

Again using $\frac{\partial^2 \delta_x}{\partial \lambda_n^2} = \frac{\partial^2 \delta_x}{\partial x^2} \left(\frac{\partial X(\lambda)}{\partial \lambda_n} \right)^2 - \frac{\partial \delta_x}{\partial X} \frac{\partial^2 X(\lambda)}{\partial \lambda_n^2}$ and $\frac{\partial^2 \delta_1}{\partial \lambda_n^2} = \frac{\partial^2 \delta_1}{\partial S_1^2}$, I_2 can be rewritten as

$$I_2 = C_{hs} \sum_{n=1}^{N} \int \left[\delta_1 \left(\frac{\partial^2 \delta_x}{\partial X^2} \left(\frac{\partial X}{\partial \lambda_n} \right)^2 - \frac{\partial \delta_x}{\partial X} \frac{\partial^2 X}{\partial \lambda_n^2} \right) + 2 \frac{\partial \delta_1}{\partial S_1} \frac{\partial \delta_x}{\partial X} \frac{\partial X}{\partial \lambda_n} + \frac{\partial^2 \delta_1}{\partial S_1^2} \delta_x \right] \lambda_n P_\lambda \, D\lambda. \tag{A9}$$

Based on the details of function $X(\lambda)$, the integrals I_1 and I_2 can further be reduced. Here we give the results for S_2 and R_1.

Case $X = S_2$: Proceeding similarly for $X(\lambda) = \sum_n \lambda_n^2$, we have, from eq. (A6) and eq. (A7),

$$I_1 = \frac{\partial}{\partial S_1} (2\gamma S_1 - \frac{1}{2} \beta N(N + 2\nu - 1)) P_2 + I_0. \tag{A10}$$

and

$$I_0 = -2C_{hs} \frac{\partial}{\partial S_2} \int \delta_1 \delta_2 \left(\sum_{m,n=1}^{N} \frac{\beta \lambda_n^2}{\lambda_n - \lambda_m} + \beta \nu \sum_{n=1}^{N} \lambda_n - 2\gamma \sum_{n=1}^{N} \lambda_n^2 \right) P_\lambda \, D\lambda. \tag{A11}$$

Using the equality $2 \sum_{m,n=1}^{N} \frac{\lambda_n^2}{\lambda_n - \lambda_m} = \sum_{m,n=1}^{N} \frac{\lambda_n^2 - \lambda_m^2}{\lambda_n - \lambda_m} = 2(N-1) \sum_n \lambda_n$, I_0 can be rewritten as

$$I_0 = -C_{hs} \frac{\partial}{\partial S_2} \int \delta_1 \delta_2 \ (2(N-1+\nu)\beta S_1 - 4\gamma S_2) P_\lambda \, D\lambda \tag{A12}$$

$$= -\frac{\partial}{\partial S_2} (2(N-1+\nu)\beta S_1 - 4\gamma S_2) P_2. \tag{A13}$$

Proceeding similarly, from eq. (A9) we have

$$I_2 = 4 \frac{\partial^2}{\partial S_2^2} I_3 - 2 \frac{\partial}{\partial S_2} (S_1 P_2) + 4 \frac{\partial^2}{\partial S_1 \partial S_2} (S_2 P_2) + \frac{\partial^2}{\partial S_1} (S_1 P_2). \tag{A14}$$

Substitution of eq.(A10) and eq.(A14) in eq.(A2) for $X = S_2$ now leads to

$$\frac{\partial P_2}{\partial Y} = 4\frac{\partial^2 (S_2\, P_2)}{\partial S_2 \partial S_1} + 4\frac{\partial^2 I_3}{\partial S_2^2} + \frac{\partial^2 (S_1\, P_2)}{\partial S_1^2} + 2\frac{\partial (Q_2\, P_2)}{\partial S_2} + \frac{\partial (Q_1\, P_2)}{\partial S_1}, \tag{A15}$$

with $Q_2 \equiv (2\gamma S_2 - \beta(N + \nu - 1)S_1 - S_1)$, $Q_1 = 2\gamma S_1 - \frac{\beta}{2}N(N + 2\nu - 1)$ and

$$I_3 = \int \prod_{k=1}^{2} \delta_{S_k} \left(\sum_n \lambda_n^3\right) P_\lambda\, \mathrm{D}\lambda = \int S_3\, P_3(S_1, S_2, S_3)\, \mathrm{d}S_3. \tag{A16}$$

Case $X = R_1$**:** Following from above, we have for $X(\lambda) = -\sum_n \lambda_n \log \lambda_n$,

$$I_1 = \frac{\partial}{\partial S_1}(2\,\gamma\, S_1 - \frac{1}{2}\beta N(N + 2\nu - 1))\, P_v(S_1, R_1, Y) + I_0, \tag{A17}$$

and

$$I_0 = C_{hs}\frac{\partial}{\partial R_1} \int \delta_1\, \delta_v \left[\sum_{m,n=1}^{N} \frac{\beta \lambda_n\, (1 + \log \lambda_n)}{\lambda_n - \lambda_m} + \beta\nu \sum_n (1 + \log \lambda_n) - 2\gamma \sum_n \lambda_n\, (1 + \log \lambda_n)\right] P_\lambda \mathrm{D}\lambda. \tag{A18}$$

Further, using the relation $\sum_{n \neq m} \frac{\lambda_n \log \lambda_n}{\lambda_n - \lambda_m} \approx \frac{N(N-1)}{2} - \frac{(N-1)}{2}R_0$ where $R_0(\lambda) \equiv -\sum_n \log \lambda_n$ (derived in *appendix J* of [17]), eq.(A18) can be rewritten as

$$I_0 = \frac{\partial}{\partial R_1} \left[\left(\beta N(N + \nu - 1) + 2\gamma(R_1 - S_1) - \beta\frac{N_\nu}{2}R_0\right) P_v\right]. \tag{A19}$$

Substitution of eq.(A17) and eq.(A19) in eq.(A6), we have for $X = R_1$,

$$\begin{aligned}
I_1 &= \frac{\partial}{\partial S_1}\left[\left(2\,\gamma\, S_1 - \frac{1}{2}\beta N(N + 2\nu - 1)\right) P_v\right] \\
&+ \frac{\partial}{\partial R_1}\left[\left(\beta N(N + \nu - 1) + 2\gamma(R_1 - S_1) - \beta\frac{N_\nu}{2}R_0\right) P_v\right].
\end{aligned} \tag{A20}$$

Substituting $X = -\sum_n \lambda_n \log \lambda_n$ in eq.(A9), I_2 can be written as

$$\begin{aligned}
I_2 &= \frac{\partial^2}{\partial R_1^2}\left((S_1 - 2R_1)P_v + J_1\right) - 2\frac{\partial^2}{\partial S_1 \partial R_1}\left((S_1 - R_1)P_v\right) \\
&+ N\frac{\partial}{\partial R_1}P_v + \frac{\partial^2}{\partial S_1^2}(S_1 P_v),
\end{aligned} \tag{A21}$$

with

$$J_k = \int \delta_{R_1} \, \delta_{S_1} \left[\sum_n (\lambda_n)^k (\log \lambda_n)^{k+1} \right] P_\lambda \, \mathrm{D}\lambda, \tag{A22}$$

where $\delta_{R_1} \equiv \delta(R_1 + \sum_n \lambda_n \log \lambda_n)$ and $\delta_{S_1} \equiv \delta(S_1 - \sum_n \lambda_n)$.

$\Rightarrow$

$$\begin{aligned}
\frac{\partial P_v}{\partial Y} &= 2 \frac{\partial^2}{\partial R_1 \partial S_1} \left[(R_1 - S_1) \, P_v \right] + \frac{\partial^2}{\partial R_1^2} \left[(S_1 - 2R_1) P_v + J_1 \right] + \frac{\partial^2}{\partial S_1^2} (S_1 \, P_v) \\
&+ \frac{\partial}{\partial R_1} \left[\left(\beta N (N + \nu - 1) + 2\gamma (R_1 - S_1) - \beta \frac{N_\nu}{2} \langle R_0 \rangle + N \right) P_v \right] \\
&+ \frac{\partial}{\partial S_1} \left[\left(2 \, \gamma \, S_1 - \frac{1}{2} \beta N N_\nu \right) P_v \right].
\end{aligned} \tag{A23}$$

To express the above integral in terms of P_v, we can approximate them as follows. We rewrite J_k as

$$J_k = \int T_k \, P(R_1, S_1, T_k) \, \mathrm{d}T_k, \tag{A24}$$

with

$$P(R_1, S_1, T_k) = \int \delta_{R_1} \, \delta_{S_1} \delta_{T_k} \, P_\lambda \, \mathrm{D}\lambda, \tag{A25}$$

and $T_k = \sum_n (\lambda_n)^k (\log \lambda_n)^{k+1}$. Using condition probability relation $P(R_1, S_1, T_k) = P(T_k | R_1, S_1) \, P(R_1, S_1)$ in eq.(A24), we have

$$J_k = P(R_1, S_1) \int T_k \, P(T_k | R_1, S_1) \, \mathrm{d}T_k, \tag{A26}$$

$$= P(R_1, S_1) \, \langle T_k \rangle_{R_1, S_1} \tag{A27}$$

We note that T_k varies very slowly with R_1 and S_1; this permits the approximation $\langle T_k \rangle_{R_1, S_1} \approx \langle T_k \rangle$.

Appendix B: Solution of eq. (21)

For large Y, $\langle S_3 \rangle$ approaches a constant: $\langle S_3 \rangle \sim \frac{1}{N^2}$. Again using separation of variables and for arbitrary initial condition at $Y = Y_0$, the solution can be given as

$$\Psi(x; Y) = \mathrm{e}^{-E \, (Y - Y_0)} \, V(x; E), \tag{B1}$$

where $V(x, E)$ is the solution of the differential equations

$$\frac{\mathrm{d}^2 V}{\mathrm{d}x^2} + 2x \frac{\mathrm{d}V}{\mathrm{d}x} + \frac{d}{2\omega} V = 0, \tag{B2}$$

with $\eta \approx 4\omega + 2\gamma \approx 4\omega$, $d = d_0 + E$ with E as an arbitrary semi-positive constant and $d_0 = (\gamma - \beta N N_\nu)\frac{\omega}{2} + \omega^2 + 4\gamma + 1$. In large N limit, d_0 can further be approximated as $d_0 \approx \frac{\omega}{2}(2\omega - \beta N N_\nu) > 0$ (assuming $\omega \gg N N_\nu, \gamma$). A solution of eq.(B2) can now be given as

$$V(x; E) = \mathrm{e}^{-x^2} \left(c_1(E) \, H_{2\mu}(x) + c_2(E) \, {}_1F_1\left(-\mu, \frac{1}{2}, x^2\right) \right), \tag{B3}$$

with $\mu = \frac{d - 4w}{8w} \approx \frac{d}{8\omega}$. The constants of integration c_1, c_2 are determined from the boundary conditions. Here $H_\mu(x)$ is the Hermite's function and ${}_1F_1(-\mu, \zeta; z)$ is the confluent Hypergeometric function defined as ${}_1F_1(-\mu, \zeta; z) = \sum_{k=0}^{\infty} \frac{(-\mu)_k z^k}{k! \zeta_k}$ with symbol $a_k \equiv \prod_{n=0}^{k-1}(a + n)$.

Further, noting that

$$H_{2\mu}(x) = \frac{2^{2\mu}\sqrt{\pi}}{\Gamma(\frac{1-2\mu}{2})} \, {}_1F_1\left(-\mu, \frac{1}{2}, x^2\right) - \frac{2^{2\mu+1}\sqrt{\pi}}{\Gamma(-\mu)} x \, {}_1F_1\left(\frac{1-2\mu}{2}, \frac{3}{2}, x^2\right),$$

eq.(B3) can be rewritten as

$$V(S_2; E) = \mathrm{e}^{-x^2} \left(c_3(E) \, {}_1F_1\left(-\mu, \frac{1}{2}, x^2\right) + c_4(E) \, x \, {}_1F_1\left(\frac{1-2\mu}{2}, \frac{3}{2}, x^2\right) \right), \tag{B4}$$

with $c_3(E) = \frac{2^{2\mu}\sqrt{\pi}}{\Gamma(\frac{1-2\mu}{2})} c_1 + c_2$ and $c_4(E) = -\frac{2^{2\mu+1}\sqrt{\pi} \, c_1}{\Gamma(-\mu)}$.

As E is an arbitrary constant and $g(S_1)$ is an arbitrary function of S_1, it is easier to write, without loss of generality, $E = |d_0| \, m = 8\omega\mu_0 m$ with m as a semi-positive integer, satisfying the condition $E \geq 0$. This gives $d = |d_0|(m + s_0))$ and thereby $\mu \equiv \mu_m = \frac{|d_0|}{8\omega}(m + s_0)$ with $s_0 = 1, 0, -1$ if $d_0 > 0, 0, < 0$ respectively. The general solution for $\Psi(x, Y)$ can now be written as

$$\Psi(x; Y) = \mathrm{e}^{-x^2} \sum_{m=0}^{\infty} \mathrm{e}^{-8\omega\mu_0 \, m \, (Y - Y_0)} \left(c_{3m} \, {}_1F_1\left(-\mu_m, \frac{1}{2}, x^2\right) + c_{4m} \, x \, {}_1F_1\left(\frac{1-2\mu_m}{2}, \frac{3}{2}, x^2\right) \right). \tag{B5}$$

Further, following the relation

$$x^2 \, {}_1F_1\left(\frac{1-\mu_m}{2}, \frac{3}{2}, x^2\right) = \frac{1}{2} \left[{}_1F_1\left(\frac{1-\mu_m}{2}, \frac{1}{2}, x^2\right) - {}_1F_1\left(-\frac{1+\mu_m}{2}, \frac{1}{2}, x^2\right) \right],$$

we have, for large μ_m, $x^2 {}_1F_1\left(\frac{1-\mu_m}{2}, \frac{3}{2}, x^2\right) \approx 0$. For $x > 0$, the contribution from the second term in eq.(B5) can then be neglected, leading to following form

$$\Psi(x; Y) \approx e^{-x^2} \sum_{m=0}^{\infty} e^{-8\omega\mu_0 m\,(Y-Y_0)} {}_1F_1\left(-\mu_m, \frac{1}{2}, x^2\right) C_m, \tag{B6}$$

with C_m as constants to be determined from initial conditions.

To proceed further, we use following relation: for $a \to \infty$, $|ph(a)| \le \pi - \delta$ and b, z fixed

$$F(-a, b, z) \sim (z/a)^{\frac{(1-b)}{2}} \frac{e^{z/2}\Gamma(1+a)}{\Gamma(a+b)} \left(J_{b-1}\left(2\sqrt{az}\right) \sum_{s=0}^{\infty} \frac{p_s(z)}{(-a)^s} - \sqrt{z/a}\, J_b\left(2\sqrt{az}\right) \sum_{s=0}^{\infty} \frac{q_s(z)}{(-a)^s} \right), \tag{B7}$$

with $p_k(z) = \sum_{s=0}^{k} \binom{k}{s}(1-b)_{k-s} z^s c_{k+s}(z)$, $q_k(z) = \sum_{s=0}^{k} \binom{k}{s}(2-b)_{k-s} z^s c_{k+s+1}(z)$, where $(k+1)c_{k+1}(z) + \sum_{s=0}^{k}\left(\frac{bB_{s+1}}{(s+1)!} + \frac{z(s+1)B_{s+2}}{(s+2)!}\right)c_{k-s}(z) = 0$. For large μ_m values, substitution of eq.(B7) in eq(B6) now leads to

$$\Psi(x; Y - Y_0) \approx e^{-\frac{x^2}{2}} \sum_{m=0}^{\infty} C_m \left(\frac{x^2}{\mu_m}\right)^{\frac{1}{4}} \mathcal{J}_m\, e^{-8\omega\mu_0 m\,(Y-Y_0)}, \tag{B8}$$

with,

$$\mathcal{J}_m = J_{-1/2}\left(2\sqrt{\mu_m x^2}\right) \sum_{s=0}^{\infty} \frac{p_s(x^2)}{(\mu_m)^s} - \sqrt{\frac{x^2}{\mu_m}}\, J_{1/2}\left(2\sqrt{\mu_m x^2}\right) \sum_{s=0}^{\infty} \frac{q_s(x^2)}{(\mu_m)^s}. \tag{B9}$$

As μ_m is large for m large (eq.(31)), eq.(B9) can further be simplified by approximations $\sum_{s=0}^{\infty} \frac{v_s(x^2)}{(\mu_m)^s} \approx \frac{v_0(x^2)}{(\mu_m)}$ with $v_s \equiv p_s$ or q_s. This along with the relations $J_{-1/2}(x) = \sqrt{\frac{2}{\pi x}}\cos x$ and $J_{1/2}(x) = \sqrt{\frac{2}{\pi x}}\sin x$ gives

$$\mathcal{J}_m \approx \left(\pi^2\mu_m x^2\right)^{-1/4} \cos\left(2\sqrt{x^2\mu_m}\right), \tag{B10}$$

where the term $\sqrt{\frac{x^2}{\mu_m}}\sin\left(2\sqrt{x^2\mu_m}\right)\left(\frac{3-x^2}{12}\right)$ is neglected.

Appendix C: Solution of eq.(54)

Using separation of variables again, a solution of eq.(54) for arbitrary initial condition at $Y = Y_0$ can be written as

$$f_{v,\omega}(R_1; Y) = e^{-E\,(Y-Y_0)}\,V(R_1; E), \tag{C1}$$

with $V(R_1, E)$ as the solution of the differential equation

$$(t - 2R_1)\,\frac{\mathrm{d}^2 V}{\mathrm{d}R_1^2} + (aR_1 + b)\,\frac{\mathrm{d}V}{\mathrm{d}R_1} + d\,V = 0, \tag{C2}$$

with $a = 2\gamma + 2\,\omega \approx 2\omega$ (assuming γ finite), $b = \beta\,(N_\nu - \nu)\,N - \frac{\beta}{2}N_\nu\,\langle R_0\rangle + N + 2\,\omega - 2\gamma - 4$ where $R_0 = -\sum \log \lambda_n$, $d = E + d_0$ and $d_0 = \frac{\beta}{2}\,\omega\,N\,N_\nu + \omega^2 + (2 - 2\gamma)\,\omega - 4$, $t = 1 + \langle T_1\rangle \sim 1 + \langle R_1\rangle^2$, $N_\nu = N + 2\nu - 1$ and E as an arbitrary positive constant determined by the initial conditions on V. A solution of eq.(C2) can now be given as

$$V(R_1; E) = \left(\frac{8x}{a}\right)^\alpha \left(c_1\,U\left[\alpha + \frac{d}{a}, \alpha + 1, x\right] + c_2\,L\left[-\left(\alpha + \frac{d}{a}\right), \alpha, x\right]\right), \tag{C3}$$

with $x \equiv -a(t - 2R_1)/4$ (used for compact writing), c_1, c_2 as unknown constants of integration, $\alpha = \frac{1}{4}(at + 2b + 4)$. Here U is a confluent Hypergeometric function of first kind, defined as

$$U(a, b, x) = \frac{\Gamma(b-1)}{\Gamma(a)}\,x^{1-b}\,{}_1F_1(a - b + 1, 2 - b, x) + \frac{\Gamma(1-b)}{\Gamma(a-b+1)}\,{}_1F_1(a, b, x),$$

with ${}_1\tilde{F}_1$ as the Hypergeometric function defined as follows: ${}_1F_1(a, b, x) = \sum_{k=0}^\infty \frac{(a)_k\,x^k}{(b)_k\,k!}$. The above definition is valid for b not an integer. Here, for b as an integer, it should be replaced by b_1 where b is integer limit of b_1. Further $L_a^b(x) \equiv L(a, b; x)$ is the associated Laguerre polynomial, defined as

$$L(a, b, x) = \frac{\Gamma(a + b + 1)}{\Gamma(a + 1)\,\Gamma(b + 1)}\,{}_1F_1(-a, b + 1, x).$$

Using the above relations, eq.(C3) can be rewritten as

$$V(R_1; E) = \left(\frac{8x}{a}\right)^\alpha \left(C_1\,{}_1F_1\left[\alpha + \frac{d}{a}, \alpha + 1, x\right] + C_2\,x^{-\alpha}\,{}_1F_1\left[\frac{d}{a}, 1 - \alpha, x\right]\right). \tag{C4}$$

Here again, with both E and ω arbitrary in eq.(C1), we can write, without loss of generality, $E = m\,|d_0|$ where m is an arbitrary non-negative integer.

In large N and ω limits, we have $a \approx 2\omega$, $b \approx \beta N N_\nu + 2\omega - \frac{\beta}{2}N_\nu\langle R_0\rangle$ with $\langle R_0\rangle \sim N \log N$ [17] , $d_0 \approx \omega\left(\frac{\beta}{2}NN_\nu + \omega\right) > 0$. The general solution can now be written as

$$f_{v,\omega}(R_1; Y) = \sum_{m=0}^{\infty} e^{-m |d_0| (Y-Y_0)} V_m(R_1; E), \tag{C5}$$

with,

$$V_m(R_1; E) = \left(\frac{4x}{\omega}\right)^{\alpha} \left(C_{1m} \, {}_1F_1\left(\alpha + \frac{d_m}{2\omega}, \alpha + 1, x\right) + C_{2m} \, x^{-\alpha} \, {}_1F_1\left(\frac{d_m}{2\omega}, 1 - \alpha, x\right)\right), \tag{C6}$$

with $x \equiv -\frac{\omega}{2}(t - 2R_1) \sim -\frac{\omega}{2}(1 + \langle R_1 \rangle^2 - 2R_1)$ and $d_m = d_0(1 + m) \approx (m + 1)\omega \left(\frac{\beta}{2}NN_\nu + \omega\right)$ and $\alpha \approx \frac{1}{2}(\omega t + b)$. Further, as the contribution from the second term in eq.(C6) is negligible as compared to first term, and we can approximate $V_m(R_1; E) = \left(\frac{4x}{\omega}\right)^{\alpha} C_{1m} \, {}_1F_1\left(\alpha + \frac{d_{m,}}{2\omega}, \alpha + 1, x\right)$

$$f_{v,\omega}(R_1; Y) = \left(\frac{4x}{\omega}\right)^{\alpha} e^x \sum_{m=0}^{\infty} C_m \, e^{-m |d_0| (Y-Y_0)} \, {}_1F_1\left(1 - \frac{d_{m,}}{2\omega}, \alpha + 1, -x\right). \tag{C7}$$

Appendix D: Calculation of variance of purity from eq.(21)

Eq.(21) describes the Y-evolution of the distribution f_2 of the purity S_2. This can further be used to derive the Y-evolution of the variance of S_2. Using the definition of variance $\langle \Delta S_2^2 \rangle \equiv \langle S_2^2 \rangle - \langle S_2 \rangle^2$ and the nth order moment as $\langle S_2^n(Y) \rangle = \int S_2^n f_2(S_2, Y) \, dS_2$ with $\int f_2 \, dS_2 = 1$, we have

$$\frac{\partial \langle \Delta S_2^2 \rangle}{\partial Y} = \frac{\partial \langle S_2^2 \rangle}{\partial Y} - 2 \langle S_2 \rangle \frac{\partial \langle S_2 \rangle}{\partial Y}, \tag{D1}$$

Substituting the definition of $\langle \Delta S_2^2 \rangle$, along with eq.(21), in the above equation, with $a = 4\langle S_3 \rangle$, $\eta \approx 4\omega$, $b = -(N_a + N_b - 1)\beta$, and repeated partial integration of the terms in right side of the above equation gives

$$\frac{\partial \langle S_2 \rangle}{\partial Y} = -b - \eta \langle S_2 \rangle \tag{D2}$$

$$\frac{\partial \langle S_2^2 \rangle}{\partial Y} = 2a - 2\eta \langle S_2^2 \rangle - 2b \langle S_2 \rangle \tag{D3}$$

Substitution of eq. (D2) and eq.(D3) in eq.(D1) then leads to

$$\frac{\partial \langle \Delta S_2^2 \rangle}{\partial Y} = 2a - 2\eta \langle \Delta S_2^2 \rangle. \tag{D4}$$

The above equation can now be solved to give

$$\langle \Delta S_2^2 \rangle = \frac{a}{\eta} - A\,e^{-2\eta Y}, \tag{D5}$$

where the constant of integration A is determined by the initial condition which is system dependent. Nonetheless, since, $\omega \sim N^2$, and $\langle S_3 \rangle \sim \frac{1}{N^2}$, we infer that in the stationary limit, $Y \to \infty$, $\langle \Delta S_2^2 \rangle \sim \frac{1}{N^4}$, verified numerically in section V.

Appendix E: Calculation of variance of von Neumann entropy from eq.(61)

With variance defined as $\langle \Delta R_1^2 \rangle \equiv \langle R_1^2 \rangle - \langle R_1 \rangle^2$ with $\langle R_1^n(Y) \rangle = \int R_1^n\, f_v(R_1, Y)\, dR_1$ with $\int f_v\, dR_1 = 1$, here again we have

$$\frac{\partial \langle \Delta R_1^2 \rangle}{\partial Y} = \frac{\partial \langle R_1^2 \rangle}{\partial Y} - 2\langle R_1 \rangle \frac{\partial \langle R_1 \rangle}{\partial Y}, \tag{E1}$$

Using the definition of $\langle R_1 \rangle$ and $\langle R_1^2 \rangle$ along with eq.(54) into above equation, with $t \approx 1 - R_1^2$, $a \approx 2w$, $b \approx \beta N(N + \nu - 1) - \beta \frac{N_\nu}{2}\langle R_0 \rangle + N + 2\omega$, and repeating the steps in the preceding section we get,

$$\frac{\partial \langle R_1 \rangle}{\partial Y} = (4 - a)\langle R_1 \rangle - (4 + b) \tag{E2}$$

$$\frac{\partial \langle R_1^2 \rangle}{\partial Y} = (6 - 2a)\langle R_1^2 \rangle - 2(4 + b)\langle R_1 \rangle + 2. \tag{E3}$$

Substitution of the above equations in eq.(E1), and, as b and a are large, we can approximate

$$\frac{\partial \langle \Delta R_1^2 \rangle}{\partial Y} = -2a\langle \Delta R_1^2 \rangle + 2, \tag{E4}$$

or,

$$\langle \Delta R_1^2 \rangle = \frac{1}{a} - Be^{-2aY}. \tag{E5}$$

That is, in the stationary limit $\langle \Delta R_1^2 \rangle \sim \frac{1}{N^2}$, which is much larger that the fluctuations in purity, which we verify numerically.